THE PROBLEM OF TWO OR MORE INDENTORS MOVING OVER THE SURFACE OF A VISCOELASTIC HALF-PLANE

by

He-zhi Fan
B.Eng., Tsinghua University, Beijing, China, 1982
M.Eng., Tsinghua University, Beijing, China, 1984

A THESIS SUBMITTED IN PARTIAL FULFILLMENT
OF THE REQUIREMENTS FOR THE DEGREE OF
DOCTOR OF PHILOSOPHY
in the Department of Mathematics & Statistics

SIMON FRASER UNIVERSITY
August 1993

APPROVAL

Name: He-zhi Fan

Degree: Doctor of Philosophy

Title of thesis: The Problem of Two or More Indentors Moving over the Surface of a Viscoelastic Half-plane

Examining Committee:

Chairman: *Dr. S.K. Thomason*

Dr. G.A.C. Graham
Senior Supervisor

Dr. M. Singh

Dr. M.R. Trummer

Dr. T. Tana

Dr. G.M.L. Gladwell
External Examiner
Professor of Civil Engineering and
Professor of Applied Mathematics
University of Waterloo, Ontario

Date Approved: August 13, 1993

PARTIAL COPYRIGHT LICENSE

I hereby grant to Simon Fraser University the right to lend my thesis, project or extended essay (the title of which is shown below) to users of the Simon Fraser University Library, and to make partial or single copies only for such users or in response to a request from the library of any other university, or other educational institution, on its own behalf or for one of its users. I further agree that permission for multiple copying of this work for scholarly purposes may be granted by me or the Dean of Graduate Studies. It is understood that copying or publication of this work for financial gain shall not be allowed without my written permission.

Title of Thesis/Project/Extended Essay

The problem of two or more indentors moving over the surface of a viscoelastic half-plane

Author: _____
(signature)

He-zhi Fan
(name)

June 21, 1993
(date)

Abstract

The problem of several indentors moving on a viscoelastic half-plane is considered in the non-inertial approximation. The solution of this mixed boundary value problem is formulated in terms of a coupled system of integral equations in space and time. These are solved numerically in the steady-state limit for the case of two indentors. The phenomena of hysteretic friction and the interaction between the two indentors are explored.

First, after the introduction in Chapter 1, the fundamental equations due to Golden and Graham based on the Kolosov-Muskhelishvili equations are given in Chapter 2 and Chapter 3. A coupled system of integral equations in space and time is finally deduced. By using the decomposition of hereditary integrals, the solutions for two and more moving loads are derived as an extension of the method for one loading treated by Golden and Graham [19].

In Chapter 4, viscoelastic material behavior is taken to be that of the standard linear solid. The steady-state limit case of the integral equations is considered. The solution for a single load due to Golden is extended to the case of two indentors. For the standard linear solid, the coupled integral equations are reduced to implicit algebraic equations with the constraint conditions. Considerable analytical progress is made before resorting to numerical techniques of solution. An expression for the hysterestic friction is also given.

The last chapter presents the numerical results. Two values of the viscous parameter $C_v = G_1/G_0$ are chosen. The kernels of the integral equations contain integrable singularities, and integrals involving them are evaluated by suitable numerical quadrature formulae and iteration schemes. The numerical results for the pressure distributions and contact regions are studied. The behaviour of the hysterestic friction and other numerical results are discussed in this chapter.

Dedication

To my family and my homeland.

Acknowledgements

I am deeply grateful to my supervisor, Dr. G.A.C. Graham, for his invaluable advice and guidance; without these this thesis would not have come into existence.

I would like to express my thanks to Dr. J.M. Golden for all of his suggestion and the time he spent on this research.

I especially thank the Department of Mathematics & Statistics, Simon Fraser University, for giving me the opportunity to study here and the financial support during my studies. Thanks are due to Mrs. S. Holmes and Mrs. M. Fankboner for their great assistance. The financial support from Dr. Graham's research grant is also appreciated.

Above all I acknowledge in all sincerity the consistent encouragement and every possible help from my wife and my family.

Contents

List of Tables

List of Figures

Chapter 1

Introduction

We consider here the moving contact problem in viscoelasticity, which is the problem of one or more indentors, or punches, pressed into a viscoelastic half-space and moving over the surface. The indentors are assumed to be infinite in one direction, with a uniform cross-section and to be parallel. Thus, plane strain conditions prevail. The material is assumed to occupy the half-space $y > 0$, and the indentors are taken to be moving in a negative x direction. To solve this problem means finding the relationship between the loads W_i which act on the ith indentor, the pressure distribution under the indentors and the contact regions C_i. Deformation or displacement derivatives may also be determined.

As Johnson [30] points out, 'the subject of contact mechanics may be said to have started in 1882 with the publication by Heinrich Hertz [25] of his classic paper *On the contact of elastic solids*'. Using certain approximations, he gave a normal pressure distribution, known as the ellipsoidal-Hertzian-distribution, as the contact area is an ellipse under his assumption. He also gave an expression for the indentation. In spite of the approximations, the theory does yield predictions which are a useful first step in the analysis of real contacting bodies. In the numerical analysis here, the Hertzian results, in their two-dimensional limit, are taken as initial data.

The Hertz contact theory is restricted to frictionless surfaces and perfectly elastic solids [30]. Progress in contact mechanics in the second half of this century has been associated

largely with the removal of these restrictions. To quote Gladwell [6], 'this theory is widely regarded as one of most beautiful and challenging fields of classical linear mechanics.' Gladwell points out that during the last hundred years it has been the cradle in which a number of powerful mathematical methods have grown. Among these are the complex variable method conceived by Kolosov and brought to maturity by Muskhelishvili [40] in the 1950's. 'Muskhelishvili's great contribution was the introduction of a systematic, direct method to replace the guess work by which the complex potentials had previously been chosen.' Such complex variable techniques, one of the most powerful methods of applied mathematics, are used here for solution of viscoelastic contact problems.

The second powerful mathematical tool which has been shaped by its use in elasticity theory is the integral transform [6]. Integral transforms were developed in piecemeal fashion during the nineteenth century but it was the seminal work of I.N. Sneddon [46] in his *Fourier Transforms (1951)* that showed they could be used for the actual solution of the difficult boundary value problems of elasticity theory. By employing the classical correspondence principle [19], some time-dependent viscoelastic equations may be reduced to standard elastic form by taking the integral transform over time t. Therefore the difficulties of such problems are no more than that for the corresponding elastic ones apart from integral transform inversion. Unfortunately this method can not be applied to all viscoelastic problems directly as there would be some points of the boundary at which the entire history of boundary conditions is unavailable. For the last three decades, work in this area has largely been devoted to such problems [19].

For a long time the mechanics of deformable bodies has been based upon Hooke's law, that is to say, upon the assumption of linear elasticity which leads to elegant mathematical structures. Almost all routine stress analysis in industry is still based on this theory. Timoshenko and Goodier [50] gave a presentation of the theory more suited to the engineer. It is well known that no mathematical theory can completely describe the complex world around us. Every theory is aimed at a certain class of phenomena, formulates their essential features, and disregards what is of minor importance. Engineers have become increasingly conscious of the importance of the inelastic behavior of many materials and mathematical formulations of this behaviour have been attempted and applied to practical problems. Outstanding among them are the theories of ideally plastic and of viscoelastic materials. While

plastic behavior is essentially nonlinear, viscoelasticity, which exhibits time-dependent behavior in the relationships between stress and strain, like elasticity, permits a linear theory. This theory of linear viscoelasticity is applied in the work here.

The earliest attempts at mathematically modeling viscoelastic behavior were those of Maxwell and Meyer [35]. Meyer's model is generally associated with the names of Kelvin and Voigt, who however made their contributions much later. This model is equivalent to simple differential constitutive relations which represent material response in the terms of springs and dashpots in series or parallel. Boltzmann [2] (1874) proposed the general hereditary integral form of the constitutive relations which is the basis of most theoretical work on viscoelastic materials of the past three decades [19]. Until the nineteen fifties, development of the subject was slow. The emergence into common use of a large variety of polymeric materials in the post-war years focussed increasing attention on the topic. The standard linear solid is a convenient non-trivial but simple model, frequently used in theoretical analysis for purposes of illustrating techniques. In the following chapters, detail about this model will be given. This was one of the special forms of the viscoelastic functions that have been found useful in practice.

There are a few books devoted exclusively to contact mechanics as Kalker [31] points out. In 1953 the book by L.A. Galin [7] appeared in Russian summarizing the pioneering work of Muskhelishvili in elastic contact mechanics. This theory is two-dimensional, considering a wide range of problems, by casting them in the form of a Riemann-Hilbert problem. Also in 1980 Galin [8] published *Contact problem in the classical theory of elasticity and viscoelasticity* which is only in Russian so far. An up-to-date and thorough treatment of same field was published in 1980 by Gladwell [7]. In 1985 Johnson's [30] book on contact mechanics appeared, in which a complete survey is given of engineering practice and concentrated on contact theory which considers contact of bodies that touch first at a point or along a line and then have a small contact patch. There is a chapter on rolling contact of elastic bodies and one on inelastic rolling contact. In Golden and Graham's [19] book, three decades of research on viscoelastic boundary value problems, mainly with moving boundary regions, are drawn together into a systematic and unified text including some new results and techniques. The plane isotherm and viscoelastic Hertz problem and its application to the impact problem are discussed, while crack and The book by Kalker [31] is the a culmination of 30 years

research by him. It represents a comprehensive account of the theories developed by himself and others to explain and predict rolling contact phenomena. Some of these theories are classical, bearing names such as Hertz, Boussinesq, Galin and Mindlin; others are at the forefront of the modeling and theory making process. A large part of the book is devoted to practical problems solved by various computer methods.

The moving boundary load problem is one typical kind of viscoelastic Hertz contact problem. The normal indentation problem is the other kind. Both involve time-dependent regions. The normal contact problem considers a rigid smooth indentor pressed into a viscoelastic half-space under varying load. Such a problem was first treated by Lee and Radok [33] in 1960, and extended by Hunter [26] and Graham [22] later. Recently, Golden and Graham [13] gave the steady-state solution to the problem subject to normal periodic loading for a standard linear solid. Lan [32] in 1991 considered this in three-dimensions for a general viscoelastic material. In this thesis the tangentially moving boundary load case is considered.

Even in a linear theory the viscoelastic moving load problem is not simple, while the theory of dry rolling contact problem for an elastic solid is now at an advanced state of development [29]. The reason for the difficulty is easy to appreciate [30]. During motion, the material lying in the front part of the contact is being compressed, while that at the rear is being relaxed. For a perfectly elastic material the deformation is reversible so that both the contact area and the stresses are symmetrical about the center line of the indentor. A viscoelastic material, on the other hand, relaxes more slowly than it is compressed so that the two bodies separate at a point closer to the center line than the point where they first make contact. The geometry of the moving contact problem in viscoelasticity is different, therefore, from that in the perfectly elastic case, and the viscoelastic solution cannot be obtained directly from the elastic solution. Furthermore the points of separation, which represent the contact region, cannot be prescribed; they have to be located from the solution process as the points where the contact pressure falls to zero, if the indentor is smooth. For two and more indentors, we need to study not only the viscoelastic effects on a particular indentor, but also the interference of viscoelastic effects from all those indentors. In other words, the history of the mixed boundary conditions, must be taken into account.

The problem of a moving indentor on a viscoelastic half-plane has received attention

for over three decades [19]. The problem of a single indentor is of considerable interest, largely because it offers a theoretical framework in which to investigate the phenomenon of hysteretic friction. If surface friction is neglected, the problem can be regarded as an indentor sliding across a lubricated half-plane, or a cylinder rolling over the plane. In 1961, Hunter [26] first presented a rigorous solution. In order to simplify the solution to the problem, the viscoelastic solid was idealized as being a standard linear material with a constant Poisson's ratio. He did this by transforming the equations into elastic form, and replacing the displacement and pressure by these quantities acted upon by differential operators. In the early work of Morland [38, 39], integral representations for the displacements and stresses were derived, leading to two pairs of linked dual integral equations for the two functions involved in the pressure representation. The method of solution, in terms of series of Bessel functions, imposed no restriction on the viscoelastic behavior. The final solution was necessarily numerical. Golden [18] presented a formalism, both simple and transparent, for this problem, with arbitrary viscoelastic behavior. The formalism, though different from that of Hunter and Morland, is related to both and clarifies the connection between the two. This method shows that the problem ultimately reduces to the solution of a linear integral equation for a quantity $v(x,t)$, closely related to the displacement outside the region of contact. This method also works well for the problem involving limiting friction [14, 17]. This moving load problem has also been considered for the transient case [12], in three-dimensions [41] and in the nonlinear case [1, 43]. Expressions were derived for the hysteretic friction in several works [14, 19, 26, 41]. General theorems concerning the existence and uniqueness of solutions to the contact problem have been given by Signorini and Fichera [4] for the elastic case and Boucher for the viscoelastic case [19].

The case of two and more moving indentors was briefly mentioned by Golden and Graham [19], but has not previously been solved. The solution of this problem will be discussed here. When there is more than one moving indentor involved there is considerable extra complexity. This is analogous to the complexity arising in vibration theory in the step from a system with a single degree of freedom to one with many. However the method used to obtain the solutions from one to two then become very relevant. We will obtain a set of coupled integral equations rather than single one.

Possible areas of practical application of the results presented here would be to wheels

on rails, the cylinder pressed against the image carrier in a printing press and so on.

The contents of this thesis are now summarized.

In Chapter 2 and Chapter 3, the fundamental equation due to Golden and Graham based on the Kolosov-Muskhelishvili equations is derived. This equation reduces to a system of coupled integral equations in space and time. The method of solution for two and more moving loads is described as an extension of the approach for dealing with one loading.

Second, in Chapter 4, viscoelastic material behaviour is taken to be that of the standard linear solid, and an expression for the hysteretic friction is given. The steady-state limit is taken in Chapter 5. The solution for a single load due to Golden is extended to the case of two indentors. For a standard linear solid, the coupled integral equations are reduced to implicit algebraic equations with the constraint conditions. Considerable analytical progress can be made before resorting to numerical techniques of solution.

Chapter 6 presents the numerical results. Two values of the viscous parameter, $C_v = G_1/G_0$, are chosen. The kernels of the integral equations contain integrable singularities, and integrals involving them are evaluated by suitable numerical quadrature formulae. Using an iteration scheme, we obtain the numerical results for the pressure distributions and contact regions. The behaviour of the hysteretic friction and other numerical results are also discussed in this chapter.

The last part contains conclusions and discussion on further work such as the case of an infinite number of indentors and the effects of inertial.

Chapter 2

The Fundamental Equations

2.1 The Moving Contact Problem

The constitutive equations of an elastic isotropic medium have the form:

$$\sigma_{ij} = 2\mu\epsilon_{ij} + \delta_{ij}\lambda\epsilon_{kk}, \tag{2.1.1}$$

where σ_{ij} and ϵ_{ij} are the stress and strain tensors which are in general functions of the position $\vec{r} = (x, y, z)$ in the material and time t. The quantities μ and λ are *Lamé*'s constants.

In a linear viscoelastic isotropic medium, the constitutive equations are replaced by

$$\sigma_{ij}(\vec{r}, t) = 2\int_{-\infty}^{t} dt'\mu(t-t')\epsilon_{ij}(\vec{r}, t') + \delta_{ij}\int_{-\infty}^{t} dt'\lambda(t-t')\epsilon_{kk}(\vec{r}, t'). \tag{2.1.2}$$

The quantities $\mu(t)$ and $\lambda(t)$, both are zero for negative t, are related to the shear and bulk relaxation moduli, $G(t)$ and $M(t)$, respectively as follows:

$$\mu(t) = \delta(t)G(0) + H(t)\frac{dG(t)}{dt} = \frac{d}{dt}[H(t)G(t)], \tag{2.1.3}$$

$$\lambda(t) = \delta(t)M(0) + H(t)\frac{dM(t)}{dt} = \frac{d}{dt}[H(t)M(t)], \tag{2.1.4}$$

where $H(t)$ is the Heaviside step function defined by

$$H(t) = \begin{cases} 0, & t < 0, \\ 1, & t \geq 0, \end{cases} \tag{2.1.5}$$

and $\delta(t)$ is the singular delta function defined by

$$\delta(t) = \begin{cases} 0, & t \neq 0, \\ \infty, & t = 0, \end{cases} \quad \text{and} \quad \int_{-\infty}^{\infty} \delta(t)dt = 1.$$

The bulk relaxation modulus $M(t)$ is simply related to the shear and volumetric relaxation moduli, $G(t)$ and $K(t)$, by

$$M(t) = K(t) - \frac{2}{3}G(t). \tag{2.1.6}$$

Taking the Fourier transforms of (2.1.2) with respect to time yields

$$\hat{\sigma}_{ij}(\vec{r},\omega) = 2\hat{\mu}(\omega)\hat{\epsilon}_{ij}(\vec{r},\omega) + \delta_{ij}\hat{\lambda}(\omega)\hat{\epsilon}_{kk}(\vec{r},\omega), \tag{2.1.7}$$

where

$$\hat{f}(\omega) = \int_{-\infty}^{\infty} dt e^{-i\omega t} f(t).$$

Note the formal identity between (2.1.7) and (2.1.1), where the complex moduli, $\hat{\mu}(\omega)$ and $\hat{\lambda}(\omega)$, play the role of *Lamé*'s constants. This is the basis of the Classical Correspondence Principle [19], which is a general method of solving viscoelastic boundary value problems. Whenever those regions over which different types of boundary conditions are specified do not vary with time, viscoelastic solutions may be generated in terms of elastic solutions that satisfy the same boundary conditions. This result may be extended in a restricted manner to problems involving time-dependent regions and is then referred to as the Extended Correspondence Principle [19].

We are considering the problem of n rigid indentors pressed into a viscoelastic half-plane ($y > 0$) and moving across it in the negative x direction. On the boundary of the $x-$axis, we denote the contact region by $c(t)$,

$$c(t) = \bigcup_{j=1}^{n} c_j(t), \quad c_j(t) = [a_j(t), b_j(t)], \quad j = 1, n, \tag{2.1.8}$$

and its complement on the boundary by $c'(t)$. The speed of the indentors is assumed to be sufficiently small for inertial effects to be neglected. The quantities, $a_j(t)$, $b_j(t)$ $j = 1, N$, are not known until the problem is solved.

The boundary conditions on the $x-$axis are formulated as follows. The displacement in the y direction is given by

$$u_2(x,t) = \begin{cases} d_j(t) - F_j(x - \bar{x}_{0j}(t)), & x \in c_j(t), \\ \text{unknown}, & x \in c'(t), \end{cases} \tag{2.1.9}$$

and the complex stress, if Coulomb's law applies, is given by

$$\Sigma(x,t) \equiv \sigma_{22} - i\sigma_{12} = \begin{cases} -(1+if)p(x), \text{ unknown}, & x \in c_j(t), \\ 0, & x \in c'(t), \end{cases} \tag{2.1.10}$$

where F_j is the shape function of the jth indentor, d_j is the displacement under the deepest point $\bar{x}_{0j}(t)$ of the indentor and f is the coefficient of friction. The displacement in the x direction is unprescribed. This is a mixed boundary value problem with moving boundary regions.

This viscoelastic moving contact problem is not amenable to solution by the Correspondence Principle[19, 20], even though some elastic solutions of the indentation problem are available in [6, 40]. The reason is simply that the boundary conditions change while the indentors are moving. The contact region, representing the part of the boundary in contact with the indentor, is unknown until the problems are solved. We have to investigate this problem directly.

2.2 Kolosov-Muskhelishvili Equations

Complex variable techniques, based on the Kolosov-Muskhelishvili (KM) equations [40], are very powerful for solving two-dimensional boundary value problems in elasticity. The viscoelastic KM equations also provide a useful starting point for considering two-dimensional viscoelastic boundary value problems and in particular plane strain problems of the kind under discussion.

Applying the theory of the biharmonic equation to the plane theory of viscoelasticity, we find that all the functions involved depend on time t as well as the complex variable $z = x + iy$ and its complex conjugate. Then the viscoelastic KM equations involve two complex potentials, $\varphi(z,t)$ and $\psi(z,t)$. For our moving contact problem, the boundary is

the x axis. Both $\varphi(z,t)$ and $\psi(z,t)$ are analytic in the upper plane $y > 0$, the domain of the material. As described in [40, 19], the latter may be eliminated and the region of analyticity of the former may be extended to the whole complex plane, by putting

$$\varphi(z,t) = -\bar{\varphi}(z,t) - z\bar{\varphi}'(z,t) - \bar{\psi}(z,t). \tag{2.2.1}$$

The bar indicates complex conjugation; over the function alone, it indicates complex conjugation, leaving z untouched; over z it affects only that quantity. In other words, if

$$F(z,t) = u(x,y,t) + iv(x,y,t)$$

then

$$\bar{F}(z,t) = u(x,-y,t) - iv(x,-y,t).$$

The KM equations, adapted in this manner, have the form

$$\sigma_{11} + \sigma_{22} = 2(\varphi(z,t) + \bar{\varphi}(\bar{z},t)) = 4Re\{\varphi(z,t)\}, \tag{2.2.2}$$

$$\Sigma(\vec{r},t) \equiv \sigma_{22} - i\sigma_{12} = \varphi(z,t) - \varphi(\bar{z},t) + (z-\bar{z})\bar{\varphi}'(\bar{z},t), \tag{2.2.3}$$

$$2\int_{-\infty}^{t} dt'\mu(t-t')D'(\vec{r},t') = \int_{-\infty}^{t} dt'\kappa(t-t')\varphi(z,t') + \varphi(\bar{z},t) + (\bar{z}-z)\bar{\varphi}'(\bar{z},t), \tag{2.2.4}$$

where the function $\varphi(z,t)$ is analytic in the whole complex plane, except on portions of the real axis. Also

$$D'(\vec{r},t) = u_1'(\vec{r},t) + iu_2'(\vec{r},t), \tag{2.2.5}$$

with the dash indicating differentiation with respect to x only and where u_1 and u_2 are the displacements in x and y directions, respectively. Also, the function $\kappa(t)$ is defined by the fact that its Fourier transformation is given, in the case of plane strain, by

$$\hat{\kappa}(\omega) = \frac{\hat{\lambda}(\omega) + 3\hat{\mu}(\omega)}{\hat{\lambda}(\omega) + \hat{\mu}(\omega)} = 3 - 4\hat{\nu}(\omega), \tag{2.2.6}$$

where $\hat{\nu}(\omega)$ is a generalized Poisson's ratio for the material.

We will sometimes refer to $\Sigma(\vec{r},t)$ and $D'(\vec{r},t)$ as the complex stress and the complex displacement derivative.

As z approaches the real axis from within the material, which is taken to be in the upper half plane, $\varphi(z,t)$ and $\varphi(\bar{z},t)$ approach $\varphi^+(x,t)$ and $\varphi^-(x,t)$, respectively, which are the limit of this complex function from above and below the x-axis.

We see from (2.2.3) that on the free boundary (regions with no stresses acting) $\varphi(z,t)$ is continuous. It is discontinuous only on regions of contact. In the case of a half plane under load, we assume that stresses and rotations vanish at infinity. Also, we assume that the boundary stresses along the x-axis fall off as $1/x^2$ or faster at large distance from the origin. Under such assumptions, $\varphi(z,t)$ behaves as $1/z$ for large $|z|$.

Methods of solution for the boundary value problems have relied heavily on analogies with elasticity. The most striking formal difference between viscoelastic equations (2.2.2) - (2.2.4) and the corresponding elastic equations is the convolution of $\kappa(t)$ and $\varphi(z,t)$ on the right of (2.2.4). Unless this can be eliminated, there is no hope of applying the standard Hilbert theory in the manner developed for elastic problems.

The obvious restriction that will remove this integral is to assume that the material possesses the proportionality property [19], from which it follows that

$$\kappa(t) = \kappa_0 \delta(t),$$

where $\kappa_0 = 3 - 4\nu_0$. Equation (2.2.4) then becomes

$$2\int_{-\infty}^{t} dt' \mu(t-t') D'(\vec{r},t') = \kappa_0 \varphi(z,t) + \varphi(\bar{z},t) + (\bar{z}-z)\bar{\varphi}'(\bar{z},t).$$

Thus, a significant mathematical simplification of the fundamental equations results from assuming that the isotropic material possesses the proportionality property. This amounts to assuming that the shear and bulk relaxation modulus, $G(t)$ and $M(t)$, or, $\mu(t)$ and $\lambda(t)$, are proportional. The latter pair is related to $G(t)$ and $M(t)$ by equations (2.1.3) and (2.1.4). Following this, it is immediate that

$$\nu(t) = \nu_0 \delta(t). \tag{2.2.7}$$

In other words, the material has a unique Possion's ratio ν_0.

The proportionality assumption means that the time behavior in shear and bulk viscoelastic functions have same shapes. However, this would not be expected to be true in general since the molecular mechanisms have little in common in these two cases. In material experiments, viscoelastic effects tend to be less pronounced for volume than for shear deformation.

This would seem to indicate that the proportionality assumption has no physical basis. But, in many cases, the bulk modulus is much larger than the shear modulus so that , for practical purposes, we can take $\nu_0 = 1/2$, as a limiting case. Also for many plastics, ν_0 is a constant but less than $1/2$, typically having values in the range $0.35 \sim 0.41$. In such cases, the proportionality assumption would seem to have approximate validity. In summary, therefore, this assumption, which is motivated primarily by the need for mathematical simplicity, is a reasonable approximation for many materials.

2.3 Hilbert Problem

Equations (2.2.3) and (2.2.4) are suitable for treating problems in which $\Sigma(\vec{r},t) = \sigma_{11} - i\sigma_{22}$ and $D'(\vec{r},t) = u' + iv'$ are known on portions of the boundary. But it is often the case that $D'(\vec{r},t)$, for example, is not known completely at any point. What is known in the contact regions is the imaginary part of $D'(\vec{r},t)$, which is the normal displacement derivative $u_2'(x,0,t)$. This means that we must take real and imaginary parts of the equations to extract the quantities that are given. This means introducing another function, namely $\bar{\varphi}(z,t)$. If the problem is then to reduce to simple Hilbert problem as we wish, it is necessary to have some relationship between $\varphi(z,t)$ and $\bar{\varphi}(z,t)$. Consider the case of limiting friction on the boundary. Since the motion is towards the negative x direction, Coulomb's Law takes the form

$$\sigma_{12}(x,t) = -f\sigma_{22}(x,t),$$

where f is the coefficient of Coulomb's friction. We deduce from (2.2.3) that

$$(1+if)\sigma_{22} = \varphi^+(x,t) - \varphi^-(x,t),$$

$$(1-if)\sigma_{22} = \bar{\varphi}^-(x,t) - \bar{\varphi}^+(x,t).$$

It follows that

$$\bar{\varphi}^+ - a\varphi^+ = \bar{\varphi}^- - a\varphi^-, \quad a = -\frac{1-if}{1+if} \tag{2.3.1}$$

at all points on the x-axis. Since $\varphi(z,t)$ is analytic in both the upper and lower half plane, except on parts of the real axis, it follows that $\bar{\varphi}(z,t)$ is also. From (2.3.1) and the fact that $\varphi(z,t) \sim 1/z$ as $|z| \to \infty$, it follows from Liouville's theorem that [19]

$$\bar{\varphi}(z,t) = a\varphi(z,t) \tag{2.3.2}$$

for all z. Using (2.3.2), we can replace equation (2.2.4) by

$$2\int_{-\infty}^{t} dt'\mu(t-t')u_2'(\vec{r},t') = \frac{1}{2i}[(1-a\kappa_0)\varphi^-(x,t) + (\kappa_0 - a)\varphi^+(x,t)] \tag{2.3.3}$$

on the boundary for a material that has the proportionality property.

If there is no friction on the boundary, $f = 0$, then $a = -1$, giving

$$\bar{\varphi}(z,t) = -\varphi(z,t), \tag{2.3.4}$$

so that (2.3.3) becomes

$$2\int_{-\infty}^{t} dt'\mu(t-t')u_2'(\vec{r},t') = \frac{1}{2i}[(1+\kappa_0)\varphi^-(x,t) + (\kappa_0 + 1)\varphi^+(x,t)], \tag{2.3.5}$$

which gives

$$\varphi^+(x,t) + \varphi^-(x,t) = i\int_{-\infty}^{t} dt' l(t-t')u_2'(x,0,t'), \tag{2.3.6}$$

where

$$l(t) = \frac{4\mu(t)}{1+\kappa_0} = \frac{\mu(t)}{1-\nu_0}. \tag{2.3.7}$$

However, in the frictionless case, it is not necessary to assume $\kappa(t) = \kappa_0\delta(t)$ [19]. One can get the same equation as above on the boundary, but where the function $l(t)$ is defined by the Fourier transform relation

$$\hat{l}(\omega) = \frac{4\hat{\mu}(\omega)}{1+\hat{\kappa}(\omega)} = \frac{\hat{\mu}(\omega)}{1-\hat{\nu}(\omega)}. \tag{2.3.8}$$

The applied stresses are zero on $c'(t)$. We only know the normal displacement derivative u_2' in $c(t)$. Under the assumption of limiting friction and $\kappa(t) = \kappa_0\delta(t)$, we have that

$$\Sigma(x,t) = -p(x,t) + is(x,t) = -(1+if)p(x,t) \tag{2.3.9}$$

where $p(x,t)$ is the normal pressure on the x-axis, $s(x,t)$ is the shear stress along the x-axis, and

$$\begin{aligned} \varphi^+(x,t) - \varphi^-(x,t) &= 0, \qquad x \in c'(t), \\ \varphi^+(x,t) - \eta\varphi^-(x,t) &= iv(x,t), \quad x \in c(t), \end{aligned} \tag{2.3.10}$$

where

$$v(x,t) = \int_{-\infty}^{t} dt' l(t-t')u_2'(x,t'), \tag{2.3.11}$$

$$l(t) = \frac{4\mu(t)}{\kappa_0 - a},$$

and

$$\eta = -\frac{1 - a\kappa_0}{\kappa_0 - a} = \frac{f + ih}{f - ih}, \qquad h = \frac{\kappa_0 + 1}{\kappa_0 - 1} = \frac{2(1 - \nu_0)}{1 - 2\nu_0}.$$

It will be convenient to put

$$\eta = e^{2\pi i\theta} \quad or$$

$$\theta = \frac{\ln \eta}{2\pi i} = \frac{1}{\pi}\tan^{-1}(\frac{h}{f}), \qquad \theta \in [0, \frac{1}{2}]. \tag{2.3.12}$$

Equations (2.3.10) define a Hilbert problem [40], the general solution of which can be written down as

$$\varphi(z,t) = \frac{X(z,t)}{2\pi}\int_{c(t)} dx' \frac{v(x',t)}{(x'-z)X^+(x',t)} + P(z,t)X(z,t) \tag{2.3.13}$$

where $P(z,t)$ is a polynomial of degree m not higher than $2n$, $c(t)$ consists of n intervals $[a_j(t), b_j(t)], j = 1, n$. There are $2n$ endpoints. We can allow the possibility of singularities at some or all of these endpoints by choosing an appropriate form of $X(z,t)$. The discussion will be confined to the case where all the indentors are smooth, so that no endpoint singularities occur. Then $m = 0$ and $P(z,t) = 0$. In this case, the quantity $X(z,t)$ has the form [19]

$$X(z,t) = \prod_{i=1}^{n}(z - a_i(t))^{1-\theta}(z - b_i(t))^{\theta}. \tag{2.3.14}$$

This function is discontinuous on $c(t)$ and continuous on $c'(t)$ and the following subsidiary conditions must be obeyed:

$$\int_{c(t)} dx \frac{x^r v(x,t)}{X^+(x,t)} = 0, \quad r = 0, n-1. \tag{2.3.15}$$

An expression for $v(x,t)$ outside of the contact region is required. Extending the second relation of (2.3.10) outside of $c(t)$ and using the first relation gives

$$iv(x,t) = (1 - \eta)\varphi(x,t), \quad or \tag{2.3.16}$$

$$v(x,t) = -2\sin(\pi\theta)e^{i\pi\theta}\varphi(x,t), \quad x \in c'(t),, \tag{2.3.17}$$

since

$$\eta = e^{i2\pi\theta}, \quad \sin(\pi\theta) = \frac{e^{i\pi\theta} - e^{-i\pi\theta}}{2i}$$

$$\frac{1-\eta}{i} = e^{i\pi\theta}\left(\frac{e^{-i\pi\theta} - e^{i\pi\theta}}{i}\right) = -2\sin(\pi\theta)e^{i\pi\theta},$$

where $\varphi(x,t)$ is the unique value of $\varphi(z,t)$ on $c'(t)$. We will also denote the unique value of $X(z,t)$ on $c'(t)$ by $X(x,t)$. More explicitly,

$$v(x,t) = \frac{-\sin(\pi\theta)e^{i\pi\theta}X(x,t)}{\pi}\int_{c(t)} dx' \frac{v(x',t)}{(x'-x)X^+(x',t)}, \quad x \in c'(t). \tag{2.3.18}$$

Also, the stresses in the contact region $c(t)$ can be written down. Note that there is discontinuity in $\varphi(z,t)$ for $x \in c(t)$. We apply the Plemelj formulas,

$$F(z) = \frac{1}{2\pi i}\int_l dt \frac{f(t)}{t-z},$$

$$F^+(x) = \frac{1}{2}f(x) + \frac{1}{2\pi i}\int_l dt \frac{f(t)}{t-x},$$

$$F^-(x) = -\frac{1}{2}f(x) + \frac{1}{2\pi i}\int_l dt \frac{f(t)}{t-x}, \quad x \in l, \tag{2.3.19}$$

where l is any smooth arc in the complex plane and the integrals in the last two relations are principal values. Substituting φ/X for F, iv/X^+ for f, and using equations (2.3.9) and (2.3.10), one can deduce that

$$\begin{aligned} \Sigma = \sigma_{22} - i\sigma_{12} \quad &= -(1+if)p(x,t) \\ = \varphi^+(x,t) - \varphi^-(x,t) \quad &= (1-1/\eta)\varphi^+ + iv/\eta, \end{aligned} \tag{2.3.20}$$

$$\varphi^+(x,t) = \frac{iv(x,t)}{2} + \frac{X^+(x,t)}{2\pi}\int_{c(t)} dx' \frac{v(x',t)}{(x'-x)X^+(x',t)}. \tag{2.3.21}$$

Then, the pressure $p(x,t)$ on the contact region is given as

$$p(x,t) = -\frac{1}{1+if}\left[\left(1-\frac{1}{\eta}\right)\frac{X^+(x,t)}{2\pi}\int_{c(t)} \frac{dx'v(x',t)}{(x'-x)X^+(x',t)} + \frac{i}{2}\left(1+\frac{1}{\eta}\right)v(x,t)\right].$$

Using

$$\frac{1}{2}\left(1+\frac{1}{\eta}\right) = \frac{e^{-i2\pi\theta}+1}{2} = \cos(\pi\theta)e^{-i\pi\theta},$$

$$\frac{1}{2}\left(1-\frac{1}{\eta}\right) = \frac{1-e^{-i2\pi\theta}}{2} = i\sin(\pi\theta)e^{-i\pi\theta},$$

we find that the above formula for the pressure $p(x,t)$ becomes

$$p(x,t) = -\frac{ie^{-i\pi\theta}}{1+if}\left[\frac{\sin(\pi\theta)X^+(x,t)}{\pi}\int_{c(t)} \frac{dx'v(x',t)}{(x'-x)X^+(x',t)} + \cos(\pi\theta)v(x,t)\right]. \tag{2.3.22}$$

It vanishes for $x \in c'(t)$.

The integrals in (2.3.21) - (2.3.22) are understood to be the Cauchy principal values [40]. When the integrands are singular in the range of integration, this will always be understood in what follows. The contact intervals $\{c(t) : [a_j(t), b_j(t)], j = 1, n\}$ are usually unknown before the problem is solved, while the overall motion of the indentors and the load on each indentor are generally specified. The loads W_j per unit length on each indentor are given by

$$W_j = \int_{a_j(t)}^{b_j(t)} dx p(x,t) = \int_{c(t)} dx J_j(x,t) v(x,t) + q \cos(\pi\theta) \int_{a_j(t)}^{b_j(t)} dx v(x,t), \tag{2.3.23}$$

where

$$J_j(x,t) = \frac{q \sin(\pi\theta)}{\pi X(x,t)} \int_{a_j(t)}^{b_j(t)} dx' \frac{X^+(x',t)}{x - x'}, \tag{2.3.24}$$

$$q = -\frac{ie^{-i\pi\theta}}{1 + if}. \tag{2.3.25}$$

This gives a total of another n conditions.

Chapter 3

Decomposition of Hereditary Integrals

For the moving indentation problem, the solutions depend on the complex potential function $\varphi(z,t)$, which is given by equation (2.3.13) under the conditions (2.3.15,2.3.23). Whenever $\varphi(z,t)$ is known, all the interesting quantities can evaluated from the KM equations, (2.2.2, 2.2.3, 2.2.4). But the complex potential function $\varphi(z,t)$ contains an unknown quantity $v(x,t)$, (2.3.11), which is known in the elastic indentation problem. In that case, $v(x,t)$ is proportional to the derivatives of the indentor profiles, since the displacement curve on the contact regions is same as the shape of indentors. In viscoelasticity, the quantity $v(x,t)$ is related to the displacement in the contact region from past to present and therefore depends on the displacement outside of contact region also. The problem is now transformed to determining the quantity $v(x,t)$.

3.1 Decomposition Method

In this section, we derive an integral equation for the quantity $v(x,t)$, $x \in c(t)$, given by equation (2.3.11) where

$$u(x,t) \equiv u_2(x,t); \quad u'(x,t) = \frac{d}{dx}u(x,t). \tag{3.1.1}$$

The function u' may be expressed as function of $v(x,t)$

$$u'(x,t) = \int_{-\infty}^{t} dt' k(t-t')v(x,t'), \tag{3.1.2}$$

where $k(t)$, $l(t)$ are two causal functions, related by

$$\int_0^t dt' k(t-t')l(t') = \int_0^t dt' l(t-t')k(t') = \delta(t), \tag{3.1.3}$$

or

$$[k * l](t) = \delta(t), \tag{3.1.4}$$

$$\hat{k}(\omega) = \frac{1}{\hat{l}(\omega)}. \tag{3.1.5}$$

Under the proportionality assumption, $l(t)$ is given in equations (2.3.11).

Let $\theta_w(x,t)$ be the set of the present and all past times, $(-\infty, t]$, which we decompose into two disjoint sets $W_u(x,t)$ and $W_\sigma(x,t)$, i.e.

$$\theta_w(x,t) = W_u(x,t) \bigcup W_\sigma(x,t), \tag{3.1.6}$$

where $W_u(x,t)$ is all those times (see figure (3.1)) $t' \leq t$ such that $x \in c(t')$ which consists of the contact regions in which the displacement in the y direction is known, and $W_\sigma(x,t)$ is all those times $t' \leq t$ such that $x \in c'(t')$ i.e. outside the contact interval in which stress distributions are known to be zero. When the jth indentor is passing point x at time t, we take the quantity $t_{2j-1}(x)$ to be the time when the front end point of first contact interval coincided with point x and $t_{2j-2}(x)$ to be the time when the rear end point of the first contact interval passed x. The point x is in $c_j(t)$, the jth contact interval at time t. Also $t_1(x)$ is the time when the front end of the jth indentor coincided with the point x. Thus, if x lies in jth contact interval,

$$W_u(x,t) = [t_{2j-1}(x), t_{2j-2}(x)] \bigcup \cdots \bigcup [t_3(x), t_2(x)] \bigcup [t_1(x), t], \tag{3.1.7}$$

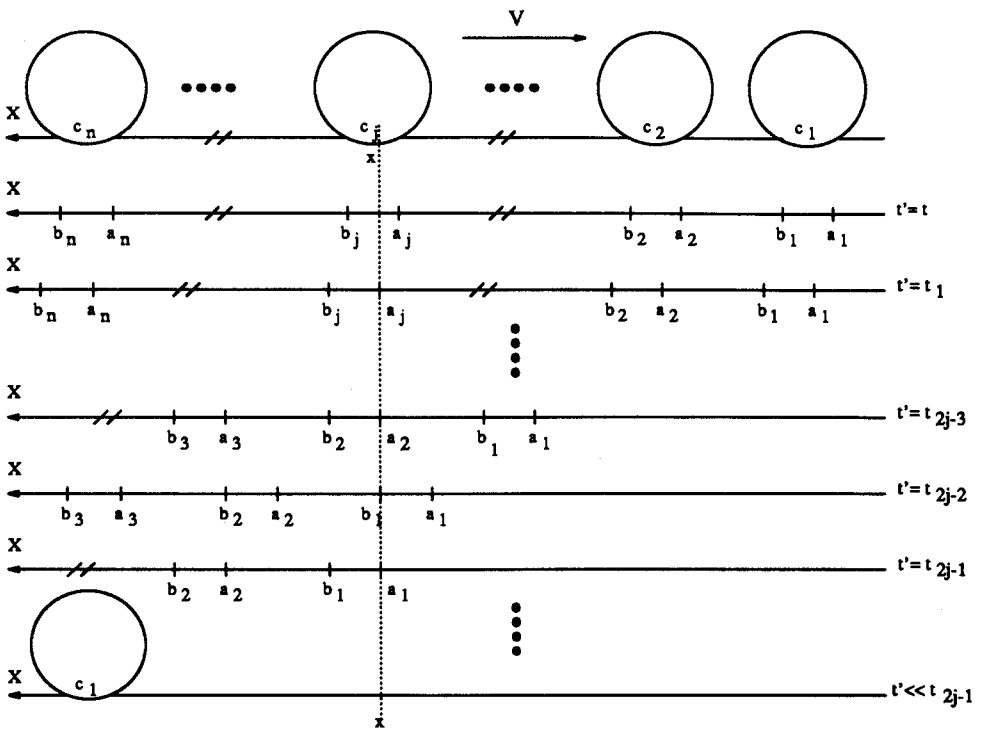

Figure 3.1: The number of the transition times and their values depend on which contact interval x belongs to. Transition times are a set of past times when the end points of the indentors passed x. Here x is in the jth contact interval $c_j(t) = [a_j(t), b_j(t)]$.

$$W_\sigma(x,t) = (-\infty, t_{2j-1}(x)) \bigcup \cdots \bigcup (t_4(x), t_3(x)) \bigcup (t_2(x), t_1(x)). \tag{3.1.8}$$

We will sometimes refer to the time $t_1(x)$, $t_2(x)$, $\cdots$ as transition times.

Now we decompose equation (2.3.11) for $v(x,t)$ when x in the contact regions by using equation (3.1.2). First we have

$$v(x,t) = \int_{t_1(x)}^{t} dt' l(t-t') u'(x,t') + \int_{-\infty}^{t_1(x)} dt' l(t-t') u'(x,t'), \quad x \in c(t), \tag{3.1.9}$$

where in the second term from equation (3.1.2)

$$u'(x,t') = \int_{-\infty}^{t'} dt k(t'-t) v(x,t). \tag{3.1.10}$$

Then carrying out an interchange of integrations, we have

$$v(x,t) = \int_{t_1(x)}^{t} dt' l(t-t')u'(x,t') + \int_{-\infty}^{t_1(x)} dt' T_1(t,t';x)v(x,t'), \tag{3.1.11}$$

where

$$T_1(t,t';x) = \int_{t'}^{t_1(x)} dt'' k(t-t'')l(t''-t').$$

The procedure can be repeated. We obtain

$$\begin{aligned} v(x,t) = &\int_{t_1(x)}^{t} dt' l(t-t')u'(x,t') + \int_{t_2(x)}^{t_1(x)} dt' T_1(t,t';x)v(x,t') \\ &+ \int_{-\infty}^{t_2(x)} dt' T_2(t,t';x)u'(x,t'), \end{aligned} \tag{3.1.12}$$

where

$$T_2(t,t';x) = \int_{t'}^{t_2(x)} dt'' T_1(t,t'';x)k(t''-t').$$

Continuing this process gives the decomposition for $x \in c(t)$ or $t \in W_u(x,t)$ [19],

$$v(x,t) = \int_{W_u} dt' \prod_u(t,t';x)u'(x,t') + \int_{W_\sigma} dt' \prod_\sigma(t,t';x)v(x,t'), \quad x \in c(t), \tag{3.1.13}$$

where

$$\begin{aligned} \prod_u(t,t';x) \quad &= T_0(t,t')R(t';t_1(x),t) \\ &+T_2(t,t';x)R(t';t_3(x),t_2(x)) \\ &+T_4(t,t';x)R(t';t_5(x),t_4(x)) \\ &+\cdots, \end{aligned} \tag{3.1.14}$$

$$\begin{aligned} \prod_\sigma(t,t';x) \quad &= T_1(t,t';x)R(t';t_2(x),t_1(x)) \\ &+T_3(t,t';x)R(t';t_4(x),t_3(x)) \\ &+T_5(t,t';x)R(t';t_6(x),t_5(x)) \\ &+\cdots, \end{aligned} \tag{3.1.15}$$

$$T_0(t,t') = l(t-t'), \tag{3.1.16}$$

$$T_j(t,t';x) = \begin{cases} \int_{t'}^{t_j(x)} dt'' T_{j-1}(t,t'';x)l(t''-t'), & \text{if } j \text{ even}, \\ \int_{t'}^{t_j(x)} dt'' T_{j-1}(t,t'';x)k(t''-t'), & \text{if } j \text{ odd}, \end{cases} \tag{3.1.17}$$

and

$$R(t;t_{k+1},t_k)=\begin{cases}1, & t\in[t_{k+1},t_k],\\ 0, & \text{otherwise},\end{cases}\quad k=1,2,\cdots. \tag{3.1.18}$$

The quantity $v(x,t')$, occurring in the second integral on the right of equation (3.1.13), is always evaluated outside of $c(t')$, by definition of $W_\sigma(x,t)$. We substitute the expression (2.3.18) for it to obtain the integral equation:

$$v(x,t)=\int_{W_\sigma(x,t)}dt'\int_{c(t')}dx'K(x,x';t,t')v(x',t')+I(x,t),\quad x\in c(t), \tag{3.1.19}$$

where

$$K(x,x';t,t')=-\frac{\sin(\pi\theta)e^{i\pi\theta}\prod_\sigma(t,t';x)X(x,t')}{\pi X^+(x',t')(x'-x)}, \tag{3.1.20}$$

$$I(x,t)=\int_{W_u(x,t)}dt'\prod_u(t,t';x)u'(x,t'). \tag{3.1.21}$$

3.2 Equations for N Moving Indentors

We now discuss this integral equation (3.1.19) in more detail for the problem of n indentors under the action of certain loads and moving across the half plane. We assume that the n indentors are all moving in the same direction, taken to be along the negative x direction for convenience.

In each interval $c_j(t)$ of the contact region

$$c(t)=\bigcup_{j=1}^{n}c_j(t),\quad c_j(t)=[a_j(t),b_j(t)],$$

we have that the displacement derivative is given by

$$u'(x,t)=f_j(x-\bar{x}_{0j}(t)),\quad x\in c_j(t),\quad j=1,n, \tag{3.2.1}$$

where the $\bar{x}_{0j}$ are the deepest points of each indentor at time t. The number of quantities $t_j(x)$, their values, and therefore W_u and W_σ depend on which contact interval x belongs to.

The intervals making up $c(t)$ are unknown before the problem is solved. They will be determined by equation (3.1.19) together with the $2n$ equations, (2.3.15) and (2.3.23). We

give the forms of W_u, W_σ and various quantities of interest for x belonging to different contact regions:

1. If x lies in the first interval $c_1(t) = [a_1(t), b_1(t)]$, there is only one transition time t_1 when the front end point $a_1(t)$ passed point x, satisfying

$$a_1(t_1(x)) = x, \qquad x \in c_1(t), \tag{3.2.2}$$

Thus, we have

$$W_u(x,t) = [t_1, t], \qquad W_\sigma(x,t) = (-\infty, t_1);$$

$$\prod_u(t,t';x) = l(t-t')R(t';t_1,t),$$

$$\prod_\sigma(t,t';x) = T_1(t,t';x)R(t';-\infty,t_1).$$

The functions $K(x,x';t,t')$ and $I(x,t)$ have the form

$$K(x,x';t,t') = K_1(x,x';t,t') = -T_1(t,t';x)Y(x,x';t')R(t';-\infty,t_1) \tag{3.2.3}$$

$$Y(x,x';t') = \frac{\sin(\pi\theta)e^{i\pi\theta}X(x,t')}{\pi X^+(x',t')(x'-x)}, \quad t' \in (-\infty, t_1) \tag{3.2.4}$$

$$I(x,t) = \int_{t_1(x)}^{t} dt' l(t-t') f_1(x - \bar{x}_{01}(t')), \tag{3.2.5}$$

and

$$v(x,t) = \int_{-\infty}^{t_1} dt' \int_{c(t')} dx' K_1(x,x';t,t')v(x',t') + I(x,t). \tag{3.2.6}$$

2. If x lies in the second interval $c_2(t) = [a_2(t), b_2(t)]$, we have

$$W_u(x,t) = [t_3, t_2] \bigcup [t_1, t],$$

$$W_\sigma(x,t) = (-\infty, t_3) \bigcup (t_2, t_1),$$

where

$$\begin{array}{lll} t_1 & \text{satisfies} & a_2(t_1(x)) = x, \\ t_2 & \text{satisfies} & b_1(t_2(x)) = x, \\ t_3 & \text{satisfies} & a_1(t_3(x)) = x, \\ \text{and} & & t_4(x) = -\infty. \end{array} \tag{3.2.7}$$

The function $K(x,x';t,t')$ takes the form

$$K(x,x';t,t') = K_1(x,x';t,t') = -T_1(t,t';x)Y(x,x';t')R(t';t_2,t_1),$$

$$t' \in (t_2, t_1), \tag{3.2.8}$$

$$K(x,x';t,t') = K_3(x,x';t,t') = -T_3(t,t';x)Y(x,x';t')R(t' : -\infty, t_3),$$

$$t' \in (-\infty, t_3), \tag{3.2.9}$$

while $I(x,t)$ is given by

$$I_2(x,t) = \int_{t_3(x)}^{t_2(x)} dt' T_2(t,t';x) f_1(x - x_{01}(t'))$$

$$+ \int_{t_1(x)}^{t} dt' T_0(t,t') f_2(x - x_{02}(t')). \tag{3.2.10}$$

The integral equation for $v(x,t)$ is given by

$$v(x,t) = \int_{-\infty}^{t_3} dt' \int_{c(t')} dx' K_3(x,x';t,t') v(x',t')$$

$$+ \int_{t_2}^{t_1} dt' \int_{c(t')} dx' K_1(x,x';t,t') v(x',t') + I(x,t). \tag{3.2.11}$$

3. For the general case, if x lies in the jth interval $c_j(t)$, we have that $W_u(x,t)$ and $W_\sigma(x,t)$ are the same as in (3.1.7) and (3.1.8), where

$$\begin{array}{lll}
t_1 & \text{satisfies} & a_j(t_1(x)) = x, \\
t_2 & \text{satisfies} & b_{j-1}(t_2(x)) = x, \\
t_3 & \text{satisfies} & a_{j-1}(t_3(x)) = x, \\
\vdots & & \\
t_{2k} & \text{satisfies} & b_{j-k}(t_{2k}(x)) = x, \\
t_{2k+1} & \text{satisfies} & a_{j-k}(t_{2k+1}(x)) = x, \quad 1 \le k < j \\
\vdots & & \\
t_{2j-1} & \text{satisfies} & a_1(t_{2j-1}(x)) = x, \\
\text{and} & & t_{2j} = -\infty.
\end{array}$$

The function $K(x,x';t,t')$ is defined by

$$K(x,x';t,t') = K_k(x,x';t,t') = -T_k(t,t';x)Y(x,x';t')R(t';t_{k+1},t_k),$$

$$t' \in (t_{k+1}, t_k),\ k = 1, 3, \cdots, 2j-1. \tag{3.2.12}$$

The function I has the form

$$I_j(x,t) = \sum_{k=1}^{j} \int_{t_{2j-2k+1}(x)}^{t_{2j-2k}(x)} dt' T_{2j-2k}(t,t';x) f_k(x - \bar{x}_{0k}(t')),$$

$$x \in c_j(t), \tag{3.2.13}$$

where $t_0 = t$. The integral equation $v(x,t)$ reads

$$v(x,t) = \sum_{k=1}^{j} \int_{t_{2k}(x)}^{t_{2k-1}(x)} dt' \int_{c(t')} dx' K_{2k-1}(x,x';t,t') v(x',t') + I_j(x,t),$$

$$x \in c_j(t). \tag{3.2.14}$$

Equation (3.1.19) involves both space and time variables occurring in an interdependent manner, which renders it unlikely that exact solutions will be available, even for simple problems. The only methods of solution, with any wide degree of applicability, would be numerical or iterative. This is for the general transient case. However, if the assumption is made that steady-state conditions prevail, the integral equation simplifies considerably. This case will be discussed later.

Chapter 4

Viscoelastic Material Response and Hysteretic Friction

4.1 Viscoelastic Material Response

4.1.1 Proportionality Assumption

In the fundamental equations, there is a convolution of $\kappa(t)$ and $\varphi(z,t)$ on the right side of (2.2.4). When we solve this set of equations, we assume that the isotropic material possesses the proportionality property [19] (see also [28]). This is a mathematical simplification, generally necessary to make any progress in solving the contact problem in viscoelasticity when friction between the half-space and the indentors is present. In the case of frictionless contact it is not necessary to make this assumption. The rationale for this assumption is briefly discussed as follows.

In linear elastic theory, the property of isotropic materials is characterized by two fundamental constants, the bulk (volume) modulus, K, and the shear modulus, G [47]. The first governs changes in size, the second, changes in shape. Their reciprocals (compliances), combinations of these, such as Poisson's ratio, ν, and other moduli can be expressed in

terms of any two of the others. In particular, every one of the constants defined as needed may be expressed in terms of the fundamental moduli, K and G, or Young's modulus, E and Poisson's ratio ν. The latter pair can be measured easily in a simple tensile test [44].

The theory of linear viscoelasticity is a generalization of linear elasticity to accommodate certain time-dependent material behavior. The various elastic constants become functions of time or, equivalently, of frequency. Just as the theory of isotropic linear elasticity involves two elastic constants, the corresponding viscoelastic theory involves two distinct transform moduli or creep functions or relaxation functions or complex moduli [28]. Several standard test procedures are described in [5, 45]. But the experiment to determine these functions is not as simple as that for elastic constants.

The proportionality assumption means that time-dependent behaviors in viscoelastic shear and bulk functions have similar shapes. In other words, the quantity $\hat{\lambda}(\omega)$ is proportional to $\hat{\mu}(\omega)$. It follows from equation (2.2.6) that assuming Possion's ratio to be a time-invariant constant is an equivalent of the proportionality assumption. Under this assumption, the property of isotropic materials in viscoelasticity is described by only one creep function or one relaxation function or one complex modulus. The rest of the moduli can be obtained from relations analogous to those in elasticity connecting the elastic constants [47].

The proportionality assumption holds for all incompressible materials. For such materials $\nu = 0.5$ and their stress-strain relation can be expressed in terms of a single function describing their behavior in shear. This is often implicit in experimental work. Many rubbers and elastomers are approximately incompressible. In small deformations of rubbers and elastomers, the values of ν range from 0.48 to 0.49 [28]. There is also the experimental result that for all but the highest frequencies, measured values of the bulk modulus $\hat{K}(\omega)$ in polymeric systems are often greater than the absolute value of the complex modulus $\hat{G}(\omega)$ by two orders of magnitude or more [5, 27]. By examing equation (2.1.6) and (2.2.6), it is seen that thses materials behavior are approximately incompressible.

Because of experimental and computational difficulties, the exact interrelations between the material functions are often difficult to obtain and use in practice. Therefore we consider approximate relations where possible. As Hunter [28] points out, solely for mathematical convenience it is often helpful to assume that $\hat{\lambda}(\omega)$ is proportional to $\hat{\mu}(\omega)$. Hunter [28] (see

also Tschoegl [52]) states that experimental evidence on the behavior of viscoelastic solids suggests that the variation of Poisson's ratio with frequency in periodic oscillations is not large. It follows that the generalized Poisson's ratio in equation (2.2.6) is approximately independent of ω;And then equation (2.2.7) holds where Poisson's ratio can be taken as a time-invariant constant, ν_0. From this, it follows that $\hat{\kappa}(\omega) = 3 - \nu_0 = \kappa_0$, which is a another equivalent of the proportionality assumption, where κ_0 is a time-invariant constant. The proportionality assumption, when $\nu_0 \neq 0.5$, is of some advantage for calculations in which it is desired to take dilatational behavior into account at least to a first approximation [27]. This assumption was discussed by Kolsky and Shi (see [27]).

In summary, therefore, the proportionality assumption, which is motivated primarily by the need for mathematical simplicity, in the frictional case, is a reasonable approximation for many materials. But we need to keep it in mind that the shear and bulk deformation are essentially different in character and accompanied by quite different molecular processes. For polymeric materials in the small-strain case, Ferry [5] points out that the complex bulk compliance is formally analogous to the complex shear compliance, but the two functions present several marked contrasts. For general materials, the appropriateness of the proportionality assumption will depend on the results of experiment. In the computation of the moving indentor problem in this thesis, the frictionless condition applied. The proportionality assumption is helpful to simplify the problem but not necessary. Without such assumption, the quantity $\hat{\mu}(\omega)/(1 - \hat{\nu}(\omega))$ appears in the frictionless case. This quantity can in the future be measured by the method outlined in [11].

4.1.2 Standard Linear Solid

In integral equation (3.1.19), the material properties in viscoelasticity are represented by the functions $l(t)$ and $k(t)$ which are two causal functions, related to each other by (3.1.5). The quantity $l(t)$ for constant Poisson's ratio, is related to the relaxation function $G(t)$. There are two categories of choices for the functions: exponential decay models and degenerate limits of these; and power law models discussed in detail in [19]. The exponential decay models emerge from the traditional mechanical models of viscoelasticity, consisting of springs and dashpots connected in series or parallel. The standard linear solid is a convenient non-trivial but simple material which contains no special degenerate features and has the

Maxwell and Voigt materials as the limiting cases.

We now specialize to the case where the material is a standard linear solid [19] with a unique Posson's ratio, which is a convenient starting point in theoretical analysis for the purposes of illustrating techniques. Its relaxation function has the form

$$G(t) = G_0 + G_1 e^{-t/\tau}, \quad t > 0, \tag{4.1.1}$$

where G_0 and G_1 are positive constants and τ is the positive decay constant. The function $\mu(t)$, from (2.1.3), has the form

$$\mu(t) = g_0\delta(t) + g_1 e^{-t/\tau} H(t), \tag{4.1.2}$$

$$g_0 = G_0 + G_1 = G(0), \tag{4.1.3}$$

$$g_1 = -G_1/\tau < 0. \tag{4.1.4}$$

Under (2.3.11), the function $l(t)$ can be shown to have a similar form to $G(t)$

$$l(t) = l_0\delta(t) + l_1 e^{-\alpha t} H(t), \tag{4.1.5}$$

where l_0, l_1 and α are given by

$$l_0 = \bar{h}(G_0 + G_1), \tag{4.1.6}$$

$$l_1 = -\bar{h}\alpha G_1 < 0, \tag{4.1.7}$$

$$\alpha = \frac{1}{\tau}, \tag{4.1.8}$$

$$\bar{h} = \frac{4}{\kappa_0 - a}. \tag{4.1.9}$$

The quantity $\bar{h}$ is complex if friction is present. In the frictionless case,

$$\bar{h} = \frac{1}{1 - \nu_0}.$$

Also, from equation (3.1.5), the function $k(t)$ can be shown to have the form

$$k(t) = k_0\delta(t) + k_1 e^{-\beta t} H(t), \tag{4.1.10}$$

where

$$k_0 = 1/l_0,$$

$$k_1 = -l_1 k_0^2,$$

$$\beta = \alpha - k_1/k_0.$$

$$\beta = \frac{1}{\tau'},$$

$$\tau' = \tau \frac{G_0 + G_1}{G_0} > \tau. \tag{4.1.11}$$

The quantity τ' is the creep function decay constant. It is always greater than the relaxation decay constant τ. We refer to the quantities α and β as inverse decay times for relaxation and creep respectively.

It is interesting to observe that if we take $\nu_0 = 1/2$, which means that the material is incompressible, then $\kappa_0 \to 1$ and

$$h = \frac{\kappa_0 + 1}{\kappa_0 - 1} \to \infty,$$

more over

$$\theta \to 1/2,$$

The solution has the same form as in the frictionless case. The effect of friction enters the equations only through the coefficient $\bar{h}$ in equation (4.1.9). This is a significant simplification.

4.2 Hysteretic Friction

The friction between sliding surfaces has two main components. The first arises from adhesion at the points where the surfaces are in molecular contact. For clean metals this adhesion may be great, as if the surfaces were welded together and the forces required to shear the junctions formed at the interface may be very large indeed no matter what load is acting on the surface. In general though, the friction is load dependent because the load determines the extent of actual contact. The second factor arises if the surface irregularities on one surface produce appreciable grooving or deformation in the other.

For most unlubricated surfaces the adhesion component dominates. In the lubricated case, the friction is very greatly reduced and its dependence on load is very different. For a

well lubricated surfaces, the friction is in fact dominated by deformation losses. Such losses, for a ball or cylinder sliding on a surface, can be estimated by comparing its rolling and sliding on same surface. When rolling, the body experiences resistance due to hysteresis losses, or in other words, those arising primarily from the viscoelastic nature of the material [48, 49]. Thus in rolling, there is no 'friction' in the conventional sense of the word – there is little shear force against the motion. Some adhesion may occur at the interface between the rolling ball and the surface, so that some work may be expended in separating the ball from the surface as rolling proceeds. This will be reduced by lubricants and its contribution to the overall rolling resistance appears, in general, to be negligible. Even in the absence of surface shear tractions, the net force on the ball or cylinder possesses a nonvanishing component opposing the forward motion. It happens as follows. The material in contact with the front portion of the contact region is compressed by the rolling ball so that work is done on it; the material in contact with the rear portion of the contact region recovers elastically and urges the ball forward. If the material were ideally elastic, the energy restored as the material recovered would be exactly equal to the energy supplied to the front portion of the region of contact and no net force would be required to roll the ball over the material. However, in practice all materials, especially polymers, lose energy when they are deformed, as a result of internal friction or hysteresis and it is this loss which is reflected in the work required to roll the ball along. Similar losses will be involved in 'frictionless' sliding, that is in sliding where interfacial adhesion is so small that no tangential force can be transmitted across the interface [24, 39].

To study the hysteretic force in moving contact problems, we first need to give an expression for the rate of energy input required to cause this movement. We consider that the indentors are in motion along the x-axis for simplicity. On the boundary, the contact region is denoted by $c(t)$, the surface tractions are the contact pressure $p(\vec{r},t)$ and the shear stress $s(\vec{r},t)$. If Coulomb's Law applies, then

$$|s(\vec{r},t)| = fp(\vec{r},t)$$

or

$$s(\vec{r},t) = sgn(U)fp(\vec{r},t), \tag{4.2.1}$$

where U is the velocity of the indentors, not necessarily constant. So, the rate of energy

input, by the moving load, is given by

$$\dot{E} = \int_{c(t)} dl(s,p) \cdot (\dot{u}_1, \dot{u}_2) = \int_{c(t)} dl[s(\vec{r},t)\dot{u}_1(\vec{r},t) + p(\vec{r},t)\dot{u}_2(\vec{r},t)], \tag{4.2.2}$$

where $u_i = u_i(\vec{r},t)$ are the surface displacements. In the one-load case, the normal displacement into the material will typically be of the form

$$u_2(\vec{r},t) = D(t) - F(\vec{r} - \vec{r}_0(t)), \quad \vec{r} \in c(t) \tag{4.2.3}$$

where $D(t)$ is the displacement under the lowest point of the indentor and F describes its profile. It is clear that F will be zero at the lowest point. The position of the lowest point is denoted as

$$\vec{r}_0(t) = (\bar{x}_0(t), 0), \quad \dot{x}_0(t) = U.$$

So, in the contact interval,

$$\dot{u}_2 = \dot{D} + U(t)\frac{\partial}{\partial x}F.$$

Then, the rate of energy input (4.2.2) is expressed by

$$\dot{E} = \int_{c(t)} dls(\vec{r},t)\dot{u}_1 + \dot{D}W(t) + \int_{c(t)} dlp(\vec{r},t)U(t)\frac{\partial}{\partial x}F, \tag{4.2.4}$$

where $W(t)$ is the total load,

$$W(t) = \int_{c(t)} dlp(\vec{r},t).$$

In the case of frictionless contact, $s(\vec{r},t) = 0$, so that

$$\dot{E} = \dot{D}W(t) + F_H U(t) sgn(U), \tag{4.2.5}$$

where F_H is the magnitude of the force resisting the horizontal motion,

$$F_H = sgn(U) \int_{c(t)} dlp(\vec{r},t)\frac{\partial}{\partial x}F.$$

The deformation caused by the moving load results in mechanical energy loss, which is manifested by the presence of a resisting force. This is just the well-known force of hysteretic friction, which is zero for a elastic material. It was demonstrated experimentally by Tabor [48, 49].

The coefficient of hysteretic friction is defined as

$$f_H = \frac{F_H}{W}. \tag{4.2.6}$$

So in the frictionless case,

$$f_H = \frac{sgn(U)}{W} \int_{c(t)} dlp(\vec{r},t) \frac{\partial}{\partial x} F.$$

If U has been constant for a long period, then steady-state conditions eventually prevail and all quantities depend on space and time coordinates only through the combination $\vec{r} - \vec{r}_0(t)$, where $\vec{r}_0(t) = (Ut, 0)$. Transferring to coordinates moving with the indentor, with the origin at the lowest point $\vec{r}_0(t)$ of the indentor, we obtain

$$p(\vec{r},t) \to p(\vec{r}), \quad F = F(\vec{r} - \vec{r}_0(t)) \to F(\vec{r}), \quad c(t) \to S, \quad \vec{r} \in S,$$

and

$$f_H = \frac{sgn(U)}{W} \int_S dlp(\vec{r}) \frac{\partial}{\partial x} F(\vec{r}). \tag{4.2.7}$$

The contact region is the region S, which is no longer time-dependent.

If the contact is frictional, we must assume to begin with that steady-state conditions apply. The reason for this is that in formula (4.2.4), we cannot otherwise be sure that $u_1(\vec{r},t)$ depends only on $\vec{r} - \vec{r}_0(t)$, which is a necessary property for the argument to go through. Under steady-state conditions, $\dot{D}$ is zero. The same argument which gave (4.2.7) now gives

$$f_H = -\frac{sgn(U)}{W} \int_S dl[s(\vec{r}) \frac{\partial}{\partial x} u_1(\vec{r}) - p(\vec{r}) \frac{\partial}{\partial x} F(\vec{r})]. \tag{4.2.8}$$

If Coulomb's Law applies, formula (4.2.8) can be simplified by using (4.2.1).

Note that there is also the ordinary frictional force

$$F_f = \int_S dls(\vec{r}) = sgn(U) fW$$

if (4.2.1) is valid, which is not shown in the rate of energy (4.2.4) at all. The formula for the hysteretic friction coefficient was given by Golden [14] and earlier authors and discussed in [19] in more detail.

Chapter 5

The Steady-state Limit

In Chapter 3 we obtained a set of coupled integral equations, (3.1.19), and conditions (2.3.15) and (2.3.23), for the moving indentor problem. The detailed form for the N moving indentor case is given in section 3.2. This is not particularly amenable to analytic treatment. The steady-state form of these equations is considerably simpler. We discuss this steady-state limit in this chapter. The term 'steady state' implies conditions of uniform motion after transient effects have died away.

5.1 Solution for a Single Load

We consider the one-indentor case first. The problem of a rigid indentor moving across a viscoelastic half-space is of considerable interest, largely because it offers a theoretical framework in which to investigate the phenomenon of hysteretic friction. Also, the solution for a single load is useful in the analysis of the multi-load case. If surface friction is neglected, the problem can be regarded as an indentor sliding across a lubricated half-plane, or a cylinder rolling over the half-plane.

This problem was first solved rigorously for a standard linear solid by Hunter [26]. He obtained the viscoelastic load-displacement equations by applying the Classical Correspondence Principle. He expressed them in a form resembling closely the differential form of the

constitutive equations for the standard linear solid, so he could apply results for the elastic indentation problem (Green & Zerna [23], for example). This procedure, Hunter found, is invalid for a more complicated solid with a number of relaxation mechanisms since the intermediate steps entail consideration of divergent integrals of type

$$\int dx' p(x') \frac{d^n}{dx^n} \log|x - x'|, \quad n > 1.$$

However, it works for $n = 1$, the case of standard linear solid, since all the integrals involved converge as Cauchy principal values.

Morland [39] considered the same problem by a different method. He formulated it as a set of dual integral equations which he then solved approximately. This approach requires no restriction on the form of the viscoelastic function though there was no question of the final results being given in analytic form. Later, Morland [37, 38], using a different technique, closer to Hunter's differential equation approach, gave a complete solution for two viscoelastic cylinders rolling on each other and also for a rigid cylinder on a viscoelastic half-plane. The viscoelastic behaviour of the material is described in term of a finite spectrum of decay times.

Golden [18] developed a general technique for solving problems of this kind and applied it to both quasi-static and inertial problems. This method, essentially that described here, is not restricted to particular types of material and works equally well for problems involving limiting friction [14, 17]. Also, the transient problem was considered by Golden and Graham [12].

As with the work of Hunter and Morland, the inertial terms are neglected here. The discussion will be confined to the steady-state problem. Figure(5.1) shows the cross-section of the moving indentor with a loading W. The contact region is $[a(t), b(t)]$.

The indentor is taken to be moving in the negative x direction with a velocity V for a long time. The deepest point of indentation is at $\bar{x}_0(t)$. We have

$$a(t) = a_0 - Vt, \quad b(t) = b_0 - Vt. \tag{5.1.1}$$

where $[a_0, b_0]$ is the initial contact interval at $t = 0$. All quantities such as u', v, p, X and so on will be the functions of $x + Vt$ rather than x, t separately. The moving indentor can be studied in a fixed coordinates, or a moving system, with $x \to y = x + Vt$. Also we choose

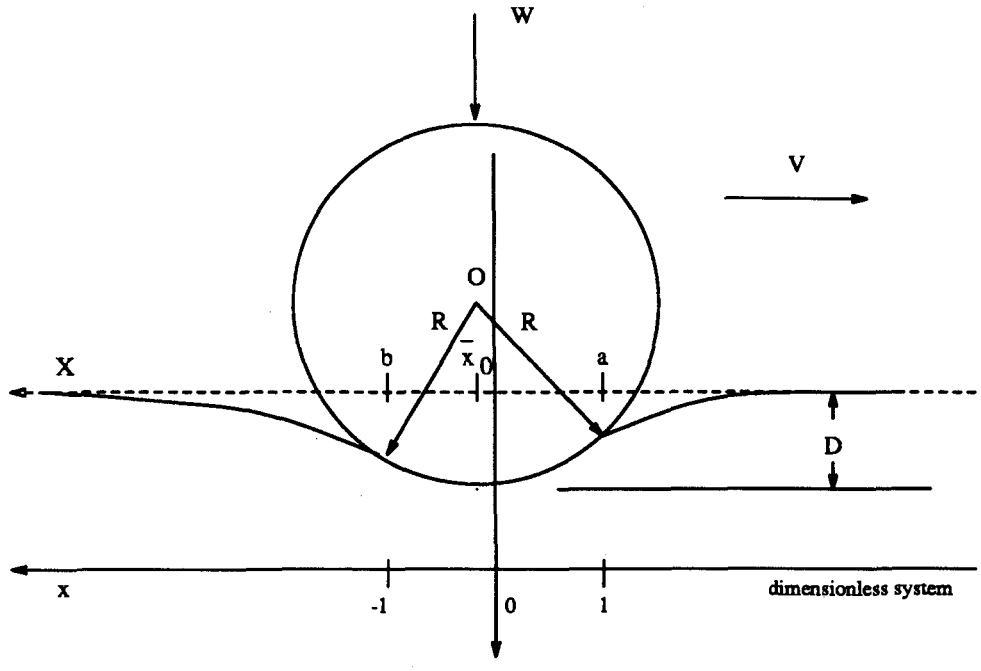

Figure 5.1: Cross section of one moving indentor.

length units and origin so that $[a_0, b_0]$ becomes $[-1, 1]$ and time units such that V becomes one. This means that a length L in the initial units, will have dimentionless length

$$l = \frac{2L - (a_0 + b_0)}{b_0 - a_0} \tag{5.1.2}$$

in the new system. Any time of duration T in the initial units becomes

$$\bar{t} = \frac{2VT}{b_0 - a_0} \tag{5.1.3}$$

in the new units. In the moving system the indentor is stationary and we refer to this system as the stationary (i.e. not time-dependent) coordinate system. The indentor is assumed to be smooth, with slope $u'(x)$ given by a polynomial,

$$u'(x) = d(x) = \sum_{r=0}^{m} d_r x^r, \tag{5.1.4}$$

where the contact region is $x \in [-1, 1]$ in the dimensionless moving coordinates mentioned above.

Equation (3.1.19) becomes [19]

$$v(x) = \int_{-1}^{1} dx' K(x,x') v(x') + I(x), \tag{5.1.5}$$

where

$$K(x,x') = \frac{\sin(\pi\theta)}{\pi} \int_{-\infty}^{-1} dy \frac{T(x,y)n(y)}{(x'-y)m(x')},$$

$$T(x,y) = \int_{y}^{-1} dy' l(x-y')k(y'-y), \quad |x| < 1, \; y < -1$$

and

$$m(x') = (x'+1)^{1-\theta}(1-x')^{\theta}, \; |x'| < 1,$$

$$n(y) = (-1-y)^{1-\theta}(1-y)^{\theta}, \; y < -1,$$

θ is given in equation (2.3.12). Also,

$$I(x) = \int_{-1}^{x} dz l(x-z)u'(z).$$

The subsidiary conditions are

$$\int_{-1}^{1} dx \frac{v(x)}{m(x)} = 0, \tag{5.1.6}$$

$$q \int_{-1}^{1} dx \frac{x v(x)}{m(x)} = W_1 = \frac{2W}{b-a}, \tag{5.1.7}$$

where

$$q = -\frac{ie^{-i\pi\theta}}{1+if}.$$

These relations determine $v(x)$ and the contact interval $[a,b]$. The quantity $\theta \to 0.5$ in the frictionless case when $f \to 0$, or for an incompressible material when $\nu \to 0.5$. Henceforth, we shall confine the discussion to the frictionless case.

We can decompose $v(x)$ into a polynomial $q(x)$ and a function $D_e(x)$, which in general has no polynomial part; in an exponential decay model, it decays exponentially with x. The polynomial $q(x)$ is given by

$$q(x) = \int_{-\infty}^{x} dx' l(x-x')d(x') = \int_{0}^{\infty} dy l(y)d(x-y) = \sum_{r=0}^{m} q_r x^r$$

In terms of Chebyshev polynomials $T_l(x)$ we have

$$\sum_{r=0}^{m} q_r x^r = \sum_{l=0}^{m} a_l T_l(x),$$

where the a_l can be determined without difficulty in any given case. The quantity $q(x)$ is known apart from the fact that it depends on the contact interval which is not given a priori, but must be determined as a result of solving the problem.

We now specialize to a particular model of viscoelastic behavior, a discrete spectrum model. The proportionality assumption will be adopted. We have for this model [19]

$$l(x) = l_0\delta(x) + \sum_{i=1}^{N} l_i e^{-\alpha_i x},$$

$$k(x) = k_0\delta(x) + \sum_{i=1}^{N} k_i e^{-\beta_i x}.$$

In the dimensionless coordinates,

$$\alpha_i = \frac{b-a}{2V\tau_i}, \quad \beta_i = \frac{b-a}{2V\tau_i'},$$

in terms of the decay constants τ_i and τ_i' for relaxation and creep respectively.

The solution of (5.1.5) has the form

$$v(x) = q(x) + D_e(x), \qquad D_e(x) = \sum_{i=1}^{N} C_i e^{-\alpha_i x},$$

where the C_i are solutions of the linear algebraic equations

$$\sum_{k=1}^{N} \frac{C_k\alpha_k\chi(\beta_j,\alpha_k)}{\alpha_k - \beta_j} = \int_{-\infty}^{-1} dy e^{\beta_j y} r(y)n(y), \tag{5.1.8}$$

$$r(y) = \sum_{l=0}^{m} a_l U_{l-1}(y),$$

$$\chi(\beta_j,\alpha_k) = -[I_0(\alpha_k)K_1(\beta_j) + I_1(\alpha_k)K_0(\beta_j)],$$

where $U_{l-1}(y)$ are Chebyshev polynomials and I_0, K_0, I_1 and K_1 are the modified Bessel functions with imaginary argument. The values of these functions can be found by referring to [36] and [53]. The system of equations (5.1.8) is essentially the form taken by (5.1.5) for a discrete spectrum material.

The subsidiary conditions, (5.1.6) and (5.1.7), become

$$\sum_{n=1}^{N} C_n I_0(\alpha_n) = -\frac{1}{\pi}\int_{-1}^{1} dx \frac{q(x)}{m(x)},$$

$$\sum_{n=1}^{N} C_n I_1(\alpha_n) = -\frac{1}{\pi}\int_{-1}^{1} dx \frac{xq(x)}{m(x)} = \frac{W_1}{\pi}. \tag{5.1.9}$$

Equations (5.1.8) together with (5.1.9) can be used to determine the constants C_k and the parameters a and b.

For a cylindrical indentor

$$d(x) = d_0 + d_1 x, \quad d_0 = -\frac{b+a}{2R}, \quad d_1 = -\frac{b-a}{2R},$$

and for a material behaving as a standard linear model ($N = 1$), equations (5.1.8) and (5.1.9) become

$$C_1 = \frac{K_1(\beta)q_1(1-\beta/\alpha)}{\beta\chi(\beta,\alpha)}, \tag{5.1.10}$$

where

$$\alpha = \frac{b-a}{2V\tau}, \ \beta = \frac{b-a}{2V\tau'}, \ 1-\beta/\alpha = \frac{G_1}{G_0+G_1},$$

and

$$q_0 = -\frac{K_1(\beta)I_0(\alpha)q_1}{\beta\chi(\beta,\alpha)}\frac{G_1}{G_0+G_1}, \tag{5.1.11}$$

$$1 + \frac{2W_1}{\pi q_1} = 2\frac{K_1(\beta)I_1(\alpha)}{\beta\chi(\beta,\alpha)}\frac{G_1}{G_0+G_1}. \tag{5.1.12}$$

Also,

$$q_0 = \frac{1}{1-\nu}(d_0 G_0 + \frac{d_1 G_1}{\alpha}),$$

$$q_1 = \frac{d_1 G_0}{1-\nu},$$

Equations (5.1.10) - (5.1.12) are equivalent to those of Hunter [26].

5.2 The Case of Two Indentors

We consider the case of two indentors, which has not been solved to date. Suppose the indentors have been moving in a negative x direction (see figure (5.2)) at the same speed V, for a long time. When transient effects have died away, then

$$a_j(t) = a_{0j} - Vt, \quad b_j(t) = b_{0j} - Vt, \quad j = 1,2. \tag{5.2.1}$$

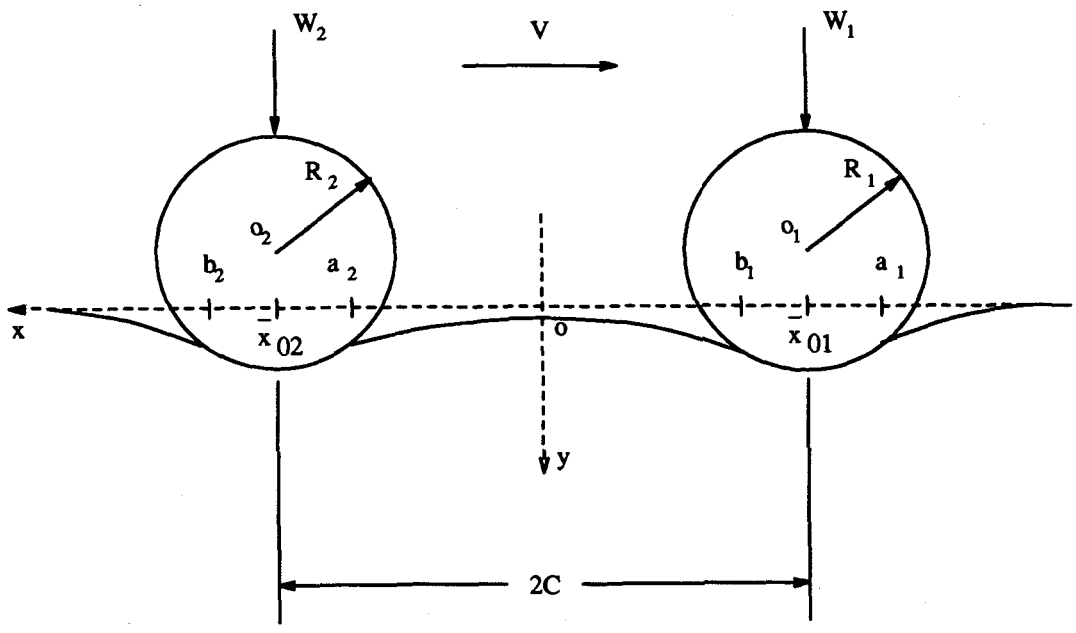

Figure 5.2: Two indentors moving along the negative direction of $x-$axis. Contact regions are $[a_1, b_1]$ and $[a_2, b_2]$. The distance between the deepest points, $\bar{x}_{01}$ and $\bar{x}_{02}$, of indentation of the two indentors is $2C$.

Introducing the variable $y = x + Vt$, we find that all physical quantities and in particular $u'(x,t)$, $v(x,t)$ and $p(x,t)$ will be functions of y rather than x, t separately. Also, the function $X(z,t)$ has the form

$$X(z,t) = (z - a_1(t))^{1-\theta}(z - b_1(t))^{\theta}(z - a_2(t))^{1-\theta}(z - b_2(t))^{\theta}, \tag{5.2.2}$$

and we can reduce $X^+(x,t)$ to $X^+(y)$, where

$$X^+(x,t) = X^+(y) = \begin{cases} m(y), & -\infty < y < a_{01}, \\ -m(y)e^{i\pi\theta}, & a_{01} \le y \le b_{01}, \\ -m(y), & b_{01} < y < a_{02}, \\ m(y)e^{i\pi\theta}, & a_{02} \le y \le b_{02}, \\ m(y), & b_{02} < y < \infty, \end{cases} \tag{5.2.3}$$

and

$$m(y) = |y - a_{01}|^{1-\theta}|y - b_{01}|^{\theta}|y - a_{02}|^{1-\theta}|y - b_{02}|^{\theta}. \tag{5.2.4}$$

Note that outside of the contact intervals, $X^-(y) = X^+(y)$, so that they can be taken as one function $X(y) = X^-(y) = X^+(y)$.

The form of the integral equation, (3.1.19), depends on which part of the contact region x belongs to, that is $[a_1(t),\ b_1(t)]$ or $[a_2(t),\ b_2(t)]$. Now, we consider in more detail how integral equation (3.1.19) in the stationary coordinates depends on the stationary contact interval which y belongs to. The stationary contact intervals are given as

$$S = S_1 \bigcup S_2, \tag{5.2.5}$$

$$S_1 = [a_{01}, b_{01}] \text{ and } S_2 = [a_{02}, b_{02}]. \tag{5.2.6}$$

First, we consider the case where y belongs to $S_1 = [a_{01}, b_{01}]$, corresponding to x belonging to $[a_1(t), b_1(t)]$. From the preceding chapter, 3, we have that the sets $W_u(x,t)$, $W_\sigma(x,t)$ are given by equations (3.1.7) and (3.1.8) From equations (3.2.2) and (5.2.1) we have

$$t_1 = \frac{a_{01} - x}{V}. \tag{5.2.7}$$

In equation (3.1.19), the functions K and I are read as

$$K(x,x';t,t') = -\frac{\sin(\pi\theta)e^{i\pi\theta}\prod_\sigma(t,t';x)X(x,t')}{\pi X^+(x',t')(x'-x)}, \tag{5.2.8}$$

$$I(x,t) = \int_{W_u(x,t)} dt' \prod_u(t,t';x)u'(x,t'). \tag{5.2.9}$$

where

$$\prod_\sigma(t,t';x) = T_1(t,t';x)R(t';-\infty,t_1(x)),$$

$$\prod_u(t,t';x) = T_0(t,t') = l(t-t'),$$

$$T_1(t,t';x) = \int_{t'}^{t_1} dt" l(t-t")k(t"-t').$$

Using stationary variables

$$u = x + Vt^* \quad z = x + Vt', \quad y = x + Vt, \tag{5.2.10}$$

we obtain from (3.1.19), the equation for $v(y)$ instead of $v(x,t)$, in stationary coordinates

$$v(y) = \int_S dy' K(y,y')v(y') + I(y), \quad y \in S_1, \tag{5.2.11}$$

$$K(y,y') = \begin{cases} K_{11}(y,y'), & y' \in S_1, \\ K_{12}(y,y'), & y' \in S_2, \end{cases} \tag{5.2.12}$$

$$K_{11}(y,y') = \frac{\sin(\pi\theta)}{\pi} \int_{-\infty}^{a_{01}} \frac{dz}{V} \frac{T_{11}(y,z)m(z)}{m(y')(y'-z)}, \tag{5.2.13}$$

$$K_{12}(y,y') = -\frac{\sin(\pi\theta)}{\pi} \int_{-\infty}^{a_{01}} \frac{dz}{V} \frac{T_{11}(y,z)m(z)}{m(y')(y'-z)}, \tag{5.2.14}$$

$$T_{11}(y,z) = \int_z^{a_{01}} \frac{du}{V} l(\frac{y-u}{V}) k(\frac{u-z}{V}), \tag{5.2.15}$$

$$I(y) = I_1(y),$$

$$I_1(y) = \int_{a_{01}}^{y} \frac{dz}{V} T_{10}(y,z) f_1(z), \quad y \in [a_{01}, b_{01}] \tag{5.2.16}$$

$$T_{10}(y,z) = l(\frac{y-z}{V}),$$

where $f_1(z)$ is the quantity defined by equation (3.2.1) in stationary coordinates.

Second, we consider the case when y lies in S_2, or x lies in $c_2 = [a_2(t), b_2(t)]$. The sets, $W_\sigma(x,t)$ and $W_u(x,t)$, are given by equations (3.1.7) and (3.1.8).

Using the conditions, (3.2.7) and (5.2.1), we get

$$t_1 = \frac{a_{02} - x}{V},$$

$$t_2 = \frac{b_{01} - x}{V},$$

$$t_3 = \frac{a_{01} - x}{V}.$$

Using the stationary variables u, z and y defined by (5.2.10), we obtain the steady state form of (3.1.19) to be in the same form as (5.2.11) but with $y \in S_2$,

$$v(y) = \int_S dy' K(y,y') v(y') + I(y), \quad y \in S_2, \tag{5.2.17}$$

$$K(y,y') = \begin{cases} K_{21}(y,y'), & y' \in S_1, \\ K_{22}(y,y'), & y' \in S_2, \end{cases} \tag{5.2.18}$$

$$K_{21}(y,y') = \frac{\sin(\pi\theta)}{\pi} [\int_{-\infty}^{a_{01}} \frac{dz}{V} \frac{T_{23}(y,z)m(z)}{m(y')(y'-z)} - \int_{b_{01}}^{a_{02}} \frac{dz}{V} \frac{T_{21}(y,z)m(z)}{m(y')(y'-z)}],$$

$$K_{22}(y,y') = -\frac{\sin(\pi\theta)}{\pi} [\int_{-\infty}^{a_{01}} \frac{dz}{V} \frac{T_{23}(y,z)m(z)}{m(y')(y'-z)} - \int_{b_{01}}^{a_{02}} \frac{dz}{V} \frac{T_{21}(y,z)m(z)}{m(y')(y'-z)}], \tag{5.2.19}$$

$$T_{20}(y,z) = l(\frac{y-z}{V}),$$

$$T_{21}(y,z) = \int_z^{a_{02}} \frac{du}{V} l(\frac{y-u}{V}) k(\frac{u-z}{V}),$$

$$T_{22}(y,z) = \int_z^{b_{01}} \frac{du}{V} T_{21}(y,u) l(\frac{y-z}{V}),$$

$$T_{23}(y,z) = \int_z^{a_{01}} \frac{du}{V} T_{22}(y,u) k(\frac{y-z}{V}), \tag{5.2.20}$$

where $T_{2i}(y,z)$, $y \in [a_{02}, b_{02}]$, i=0, 3, are derived from $T_0(t,t')$, $T_1(t,t';x)$, $T_2(t,t';x)$ and $T_3(t,t';x)$, $x \in [a_2(t), b_2(t)]$, respectively.

For the standard linear solid described in section 4.1, using the property of $\delta(t)$ and $H(t)$ and noting in S_1, $y > a_{01}, y > z$ always, we find that

$$T_{10}(y,z) = l_0 \delta(\frac{y-z}{V}) + l_1 \exp\{-\alpha \frac{y-z}{V}\}, \tag{5.2.21}$$

$$T_{11}(y,z) = k_0 l_1 \exp\{-\alpha \frac{y-a_{01}}{V} - \beta \frac{a_{01}-z}{V}\}, \tag{5.2.22}$$

for $y \in S_1$. In the same way, when $y \in S_2$, we have,

$$T_{20}(y,z) = l_0 \delta(\frac{y-z}{V}) + l_1 \exp\{-\alpha \frac{y-z}{V}\}, \tag{5.2.23}$$

$$T_{21}(y,z) = k_0 l_1 \exp\{-\alpha \frac{y-a_{02}}{V} - \beta \frac{a_{02}-z}{V}\}, \tag{5.2.24}$$

$$T_{22}(y,z) = l_1 \exp\{-\alpha \frac{y-a_{02}}{V} - \beta \frac{a_{02}-b_{01}}{V} - \alpha \frac{b_{01}-z}{V}\}, \tag{5.2.25}$$

$$T_{23}(y,z) = k_0 l_1 \exp\{-\alpha \frac{y-a_{02}}{V} - \beta \frac{a_{02}-b_{01}}{V} - \alpha \frac{b_{01}-a_{01}}{V} - \beta \frac{a_{01}-z}{V}\}. \tag{5.2.26}$$

From these expressions for T_{ij}, the functions K_{ij} can be determined. But we note that K_{ij} have infinite range integral terms like

$$\int_{-\infty}^{b} ds e^{\beta s} g(s), \quad \beta > 0.$$

which may be evaluated by the method mentioned in section 5.3.

In equation (5.2.17), $I(y) = I_2(y)$,

$$I_2(y) = \int_{a_{01}}^{b_{01}} \frac{dz}{V} T_{22}(y,z) f_1(z) + \int_{a_{02}}^{y} \frac{dz}{V} T_{20}(y,z) f_2(z), \quad y \in [a_{02}, b_{02}], \tag{5.2.27}$$

where $f_1(z)$ and $f_2(z)$ are the functions (3.2.1) evaluated in the stationary coordinate system.

Conditions (2.3.15) become

$$\sum_{j=1}^{2} \int_{S_j} dy \frac{v(y)}{m_j(y)} = 0,$$

$$\sum_{j=1}^{2} \int_{S_j} dy \frac{yv(y)}{m_j(y)} = 0, \tag{5.2.28}$$

where

$$m_j(y) = (-1)^j m(y), \quad y \in S_j,\ j = 1, 2.$$

The pressure in the stationary contact region is

$$p(y) = q[\frac{\sin(\pi\theta)X^+(y)}{\pi} \int_S dy' \frac{v(y')}{(y'-y)X^+(y')} + \cos(\pi\theta)v(y)], \tag{5.2.29}$$

where

$$q = -\frac{ie^{-i\pi\theta}}{1+if}.$$

The load subsidiary conditions, (2.3.23), are given as,

$$W_j = \int_{S_j} dyp(y) = \int_S dy' J_j(y')v(y') + q\cos(\pi\theta) \int_{a_{0j}}^{b_{0j}} dyv(y), \quad j = 1, 2, \tag{5.2.30}$$

where

$$J_j(y') = \frac{q\sin(\pi\theta)}{\pi X^+(y')} \int_{a_{0j}}^{b_{0j}} dy \frac{X^+(y)}{(y'-y)}.$$

Thus once the quantity $v(y), y \in S$ and the extent of S itself are known, other quantities of interest can be determined. The central problem is therefore the determination of $v(x)$ and S.

5.3 Computational Method

In the case of two indentors moving on the viscoelastic half plane, in the steady-state limit, the problem reduces to an integral equation for $v(y)$,

$$v(y) = \int_S dy' K(y, y')v(y') + I(y), \quad y \in S = [a_{01}, b_{01}] \bigcup [a_{02}, b_{02}] \tag{5.3.1}$$

where the kernel function $K(y, y')$ can be written as,

$$K(y,y') = \begin{cases} K_{11}(y,y'), & y \in [a_{01}, b_{01}],\ y' \in [a_{01}, b_{01}] \\ K_{12}(y,y'), & y \in [a_{01}, b_{01}],\ y' \in [a_{02}, b_{02}] \\ K_{21}(y,y'), & y \in [a_{02}, b_{02}],\ y' \in [a_{01}, b_{01}] \\ K_{22}(y,y'), & y \in [a_{02}, b_{02}],\ y' \in [a_{02}, b_{02}], \end{cases} \tag{5.3.2}$$

$$I(y) = \begin{cases} I_1(y), & y \in [a_{01}, b_{01}], \\ I_2(y), & y \in [a_{02}, b_{02}], \end{cases} \tag{5.3.3}$$

as discussed in preceding section. All the K_{ij} have the same factor $\sin(\pi\theta)/\pi$ and are in integral forms. The stationary contact intervals are usually smaller than the distance $2C = \bar{x}_{02} - \bar{x}_{01}$ between the two indentors.

It may be pointed out that the kernels of (5.3.1) possesses no non-integrable singularities. One perceives that the only situations where singularities might arise are when y' is equal to one of the stationary end points a_{0i} or $b_{0i}, i = 1, 2$. The regions of integration for $K(y, y')$ are such that y, y' cannot in general become equal. There is another source of difficulty, though. The factor $m(y')$ in the denominator of $K(y, y')$, may cause an integrable singularity in the kernel. This does not necessarily render the equation singular, however, the singularity can be transformed away by a change of variable as we can see in a worked-out example by Golden and Graham (1988).

Integral equation (5.3.1) can be regarded as a Fredholm Equation of the second kind:

$$\varphi(x) = f(x) + \lambda \int_a^b dt K(x,t)\varphi(t), \tag{5.3.4}$$

even though the region of integration, or say the domain of the unknown function $v(y)$ is over two intervals not only one. Also the intervals are unknown before the problem is solved. Some subsidiary conditions are required to determine the ends of interval. They are given in the previous section.

The task of numerically solving integral equation (5.3.1) subject to the subsidiary conditions, (5.2.28) and (5.2.30), is clearly a substantial undertaking. It will be regarded as the limiting form as $n \to \infty$ of a set of n linear algebraic equations:

$$v(y_r) = I(y_r) + \sum_{s=1}^{n} K(y_r, y_s)v(x_s)w_s\delta_s, \quad r = 1, n, \tag{5.3.5}$$

where δ_s are the subinterval lengths, $\delta_s \to 0$ as $n \to \infty$; x_r are quadrature points; w_s are quadrature weights.

Now, faced with a choice of a suitable numerical quadrature formula, balance between convenience and efficiency, and then may use the simplest quadrature rules which are adequate. Our choice could be the repeated Trapezoid or Simpson's rule because they are familiar and trivial to program. Noting however that the ends of the contact regions may have integrable singularities (transformable), we need consider the mid-point rule to avoid evaluating the integrands at the end-points of the intervals.

There are also infinite range integrals which require special consideration. Given the behaviour of $K(y, y')$, which mostly depends on the material functions $l(y), k(y)$, with their exponential decay, we may use brute force truncation of the range:

$$I = \int_{-\infty}^{a} ds f(s) \Rightarrow I_R = \int_{-R}^{a} ds f(s), \tag{5.3.6}$$

where R is finite and 'large'.

If convergence on the infinite range result is very slow, better techniques should be chosen. The most commonly used of these are the Gauss-Laguerre and Gauss-Hermite rule, or more generally, the mapped finite range rules [3, 9, 10, 42]. Such techniques can be expected to be cheaper than the crude 'truncation interval' approach also.

Chapter 6

Computational Results

6.1 Detailed Equations

6.1.1 Dimensionless coordinates for The Two-indentor Case

It is convenient to consider the moving indentor problem in a dimensionless system. Take the deepest points of indentation of the two indentors (see figure(5.2)) $\bar{x}_{01}(t)$ and $\bar{x}_{02}(t)$, respectively. They satisfy

$$\bar{x}_{0j}(t) = x_{0j} - Vt.$$

Let

$$x_{02} - x_{01} = 2C, \tag{6.1.1}$$

$$x_{01} + x_{02} = x_p, \tag{6.1.2}$$

so that the two indentors are a distance $2C$ apart. The quantity x_p can be chosen arbitrarily. We take it to be zero.

We choose length units and origin so that,

$$x_{01} \Rightarrow -1.0, \quad x_{02} \Rightarrow 1.0,$$

and time unit such that the speed V of the indentors in this new system will be 1. We obtain that any quantity of dimension length, which has value of coordinate $x = L$ in the initial system, becomes l, where

$$l = \frac{L}{C}, \tag{6.1.3}$$

and any time in the theory of value T in the initial system becomes $\bar{t}$, where

$$\bar{t} = \frac{T}{\lambda}, \quad \lambda = \frac{C}{V}, \tag{6.1.4}$$

in this dimensionless system.

In the new system, the stationary contact regions will be

$$s = s_1 \bigcup s_2, \quad s_1 = [A_1, B_1], \quad s_2 = [A_2, B_2]. \tag{6.1.5}$$

and one can set

$$D_1 = \frac{b_{01} - a_{01}}{C} = B_1 - A_1, \quad D_2 = \frac{b_{02} - a_{02}}{C} = B_2 - A_2, \tag{6.1.6}$$

which are the contact interval lengths in the dimensionless system.

It should be noted that the lengths of the contact intervals, $(b_{01} - a_{01})$ or $(b_{02} - a_{02})$, are small compared with radii, R_j, $j = 1, 2$, of the indentors. So, D_1 and D_2 should be small quantities compared with R_j/C. For the two-indentor case $(D_1 + D_2)/2$ should be less than 2, the dimensionless distance between the centers of the indentors. This means that the contact regions cannot overlap. Further we assume that the length of the free boundary between the indentors, $A_2 - B_1$, must be larger than the length of each contact region.

The inverse decay times in dimensionless coordinates are

$$\alpha = \frac{\lambda}{\tau}, \quad \lambda = \frac{C}{V}, \tag{6.1.7}$$

$$\beta = \frac{\lambda}{\tau'}. \tag{6.1.8}$$

The integral equation for $v(y)$ in dimensionless coordinates is

$$v(y) = \int_s dy' K(y, y') v(y') + I(y) \qquad y', y \in s = s_1 \bigcup s_2, \tag{6.1.9}$$

where $K(y, y')$ is equal to

$$K_{11}(y, y') = \frac{\sin(\pi\theta)}{\pi} \int_{-\infty}^{A_1} dz \frac{T_{11}(y, z) m(z)}{m(y')(y' - z)},$$

$$y \in s_1, y' \in s_1, \tag{6.1.10}$$

$$K_{12}(y,y') = -K_{11}(y,y'),\ y \in s_1, y' \in s_2, \tag{6.1.11}$$

$$K_{21}(y,y') = \frac{\sin(\pi\theta)}{\pi}\left[\int_{-\infty}^{A_1} dz \frac{T_{23}(y,z)m(z)}{m(y')(y'-z)} - \int_{B_1}^{A_2} dz \frac{T_{21}(y,z)m(z)}{m(y')(y'-z)}\right],\ y \in s_2, y' \in s_1, \tag{6.1.12}$$

$$K_{22}(y,y') = -K_{21}(y,y'),\ y \in s_2, y' \in s_2, \tag{6.1.13}$$

where the quantity $m(y)$ now has the form

$$m(y) = |y-A_1|^{1-\theta}|y-B_1|^{\theta}|y-A_2|^{1-\theta}|y-B_2|^{\theta} \tag{6.1.14}$$

For a standard linear solid (section 4.1), the T_{ij} in dimensionless system are obtained from (5.2.21) to (5.2.26) as follows:

when $y \in s_1$,

$$T_{10}(y,z) = l_0\delta(y-z) + l_1 e^{-\alpha(y-z)}, \qquad z \in s_1, \tag{6.1.15}$$

$$T_{11}(y,z) = k_0 l_1 e^{-\alpha(y-A_1)}e^{\beta(z-A_1)}, \quad z < A_1; \tag{6.1.16}$$

when $y \in s_2$,

$$T_{20}(y,z) = l_0\delta(y-z) + l_1 e^{-\alpha(y-z)}, \qquad z \in s_2, \tag{6.1.17}$$

$$T_{21}(y,z) = k_0 l_1 e^{-\alpha(y-A_2)}e^{\beta(z-A_2)}, \quad B_1 < z < A_2, \tag{6.1.18}$$

$$T_{22}(y,z) = l_1 e^{(\alpha-\beta)(A_2-B_1)}e^{-\alpha(y-z)}, \qquad z \in s_1, \tag{6.1.19}$$

$$T_{23}(y,z) = k_0 l_1 e^{-\alpha(y-A_2)}e^{\beta(z-A_1)}e^{-\alpha D_1}e^{-\beta(A_2-B_1)}, \quad z < A_1, \tag{6.1.20}$$

where l_0, l_1, k_0 and $\bar{h}$ are given by (4.1.6) - (4.1.9).

Using these relations, we can simplify the equations for $K_{ij}(y,y')$ given by (6.1.10) - (6.1.13) to

$$\hat{K}_{11}(y,y') = C_{11}e^{-\alpha(y-A_1)}\frac{J_{11}(y')}{m(y')}, \quad y \in s_1, y' \in s_1, \tag{6.1.21}$$

$$\hat{K}_{12}(y,y') = C_{12}e^{-\alpha(y-A_1)}\frac{J_{12}(y')}{m(y')}, \quad y \in s_1, y' \in s_2, \tag{6.1.22}$$

$$\hat{K}_{21}(y,y') = C_{21}e^{-\alpha(y-A_2)}\frac{C_0 J_{11}(y') - J_{21}(y')}{m(y')}, \quad y \in s_2, y' \in s_1, \tag{6.1.23}$$

$$\hat{K}_{22}(y,y') = C_{22}e^{-\alpha(y-A_2)}\frac{C_0 J_{12}(y') - J_{22}(y')}{m(y')}, \quad y \in s_2, y' \in s_2, \tag{6.1.24}$$

where

$$C_{11} = C_{21} = \frac{\sin(\pi\theta)}{\pi} k_0 l_1,$$

$$C_{12} = C_{22} = -C_{11},$$

$$C_0 = e^{-\alpha D_1 - \beta(A_2 - B_1)}, \tag{6.1.25}$$

$$J_{11}(y') = \int_{-\infty}^{A_1} dz \frac{e^{\beta(z-A_1)} m(z)}{y' - z}, \quad y' \in s_1, \tag{6.1.26}$$

$$J_{12}(y') = J_{11}(y'), \quad if\ y' \in s_2, \tag{6.1.27}$$

$$J_{21}(y') = \int_{B_1}^{A_2} dz \frac{e^{\beta(z-A_2)} m(z)}{y' - z}, \quad y' \in s_1, \tag{6.1.28}$$

$$J_{22}(y') = J_{21}(y'), \quad if\ y' \in s_2. \tag{6.1.29}$$

In the integrand of $J_{ij}, i, j = 1, 2$, a singularity may arise if y' equal to one of the end points, but it is integrable as will be shown later.

For a standard linear solid, from equations (5.2.16) and (5.2.27), I(y) is given by

$$I_1(y) = l_1 \int_{A_1}^{y} dz e^{\alpha(z-y)} f_1(z) + l_0 f_1(y), \quad y \in s_1, \tag{6.1.30}$$

$$I_2(y) = l_1 \int_{A_2}^{y} dz e^{\alpha(z-y)} f_2(z) + I_{12}(y) + l_0 f_2(y), \quad y \in s_2, \tag{6.1.31}$$

$$I_{12}(y) = l_1 e^{(\alpha-\beta)(A_2 - B_1)} \int_{A_1}^{B_1} dz e^{\alpha(z-y)} f_1(z), \tag{6.1.32}$$

There is a simple example in which the slopes of the indentor profiles are given as

$$f_1(y) = -\frac{C}{R_1}(y + 1), \quad y \in s_1,$$

$$f_2(y) = -\frac{C}{R_2}(y - 1), \quad y \in s_2, \tag{6.1.33}$$

which is an approximate model of cylinders, where the lengths of the dimensionless contact intervals, D_1 and D_2, are small compared with the dimensionless radius R_j/C of the cylinders, respectively. Alternatively, the indentors can be regarded as two parabolas.

For this case, the elastic solutions are given as follows [6]. For the single parabolic indentor,

$$f(y) = -\frac{C}{R} y,$$

the contact pressure distribution has the form

$$p(y) : \frac{p(y)}{GR} = \frac{C}{R^2(1-\mu)}\sqrt{a_0^2 - y^2},$$

where the semi-contact length a_0 satisfies the equation, which is related to the total load W,

$$\frac{W}{GR} = \frac{\pi a_0^2}{2(1-\mu)}(\frac{C}{R})^2. \tag{6.1.34}$$

The elastic solutions are important as baseline data for the viscoelastic solutions.

Let us now discuss the singularities in the integral J_{ij} in detail. We take

$$y' = \delta + A_1, \quad if\ y' \in s_1, \quad y' = \delta + A_2, \quad if\ y' \in s_2,$$

where δ will be a small quantity of the same order as $D_i, i = 1, 2$. In J_{ij}, we change the integration variable z to t, according to

$$z = A_1 - t,$$

which gives

$$y' - z = t + \delta, \quad if\ y' \in s_1, \quad y' - z = t + \delta, \quad if\ y' \in s_1,$$

$$\begin{aligned} m(z) = m^*(t) &= t^{1-\theta}(t + D_1)^\theta(t + A_2 - A_1)^{1-\theta}(t + B_2 - A_1)^\theta \\ &= t(1 + \frac{D_1}{t})^\theta(t + A_2 - A_1)(1 + \frac{D_2}{t + A_2 - A_1})^\theta, \end{aligned}$$

$$J_{11}(y') = J_{11}^*(\delta) = \int_0^\infty dt e^{-\beta t}\frac{m^*(t)}{t + \delta},$$

$$J_{12}(y') = J_{12}^*(\delta) = \int_0^\infty dt e^{-\beta t}\frac{m^*(t)}{t + A_2 - A_1 + \delta}.$$

Taking

$$D = \max\{D_1, D_2\},$$

where D_1 and D_2 are given by (6.1.6), and A is chosen as a constant such that $D/A << 1$. Then

$$\frac{m^*(t)}{t + \delta} \xrightarrow{t \geq A} t + A_2 - A_1,$$

$$\frac{m^*(t)}{t + A_2 - A_1 + \delta} \xrightarrow{t \geq A} t,$$

So we may evaluate J_{11} and J_{12} as follows

$$J_{11}(\delta) = \int_0^A dt e^{-\beta t} \frac{m^*(t)}{t+\delta} + \frac{e^{-\beta A}}{\beta}(A + A_2 - A_1 + \frac{1}{\beta})(1 + o(D/A)), \tag{6.1.35}$$

$$J_{12}(\delta) = \int_0^A dt e^{-\beta t} \frac{m^*(t)}{t + A_2 - A_1 + \delta} + \frac{e^{-\beta A}}{\beta}(A + \frac{1}{\beta})(1 + o(D/A)), \tag{6.1.36}$$

where the region of the integration is reduced from the infinite interval to $[0, A]$.

There is a singularity in the integrand of T_{11} at $t = 0$ if $\delta = 0$. However, it is obviously integrable because

$$\int_0^\epsilon dt e^{-\beta t} \frac{m^*(t)}{t+\delta} \overset{\delta=0, \epsilon << min\{1, D_1\}}{\longrightarrow} \int_0^\epsilon dt \frac{C^*}{t^\theta},$$

where C^* is some constant. This exists since $\theta \in [0, 1/2]$. Singularities arise in the integrand of J_{21} when $y' = z = B_1$ and J_{22} when $y' = z = A_2$. In both cases, J_{21} and J_{22} are integrable too.

For these integrable quantities, we can use a suitable numerical quadrature formula. For example, we can use the right-end point rule or mid-point rule to evaluate J_{11}, J_{12} or J_{21} and the left-end point rule or mid-point rule for J_{22}.

In the dimensionless system, the solvability conditions (5.2.28) take the same form as (5.2.28) but evaluated in dimensionless region s

$$\sum_{j=1}^{2} \int_{s_j} dy \frac{v(y)}{m_j(y)} = 0,$$

$$\sum_{j=1}^{2} \int_{s_j} dy \frac{yv(y)}{m_j(y)} = 0. \tag{6.1.37}$$

The pressure in the contact region is given by (5.2.29) but now evaluated over the dimensionless region s.

The expression for the pressure is

$$p(y) = \begin{pmatrix} p_1(y) \\ p_2(y) \end{pmatrix}, \quad y \in s_i, i = 1, 2,$$

$$p_i(y) = h_q[\frac{\sin(\pi\theta) m_i(y)}{\pi} \sum_{j=1}^{2} \int_{s_j} dy' \frac{w(y')}{(y'-y) m_j(y')} + \cos(\pi\theta) w(y)],$$

$$y \in s_i, i = 1, 2, \tag{6.1.38}$$

where

$$h_q = -\frac{4\sin(\pi\theta)}{\kappa + 1} = -\frac{\sin(\pi\theta)}{1 - \nu}.$$

and $w(y)$ is a real function such that

$$v(y) = \bar{h} w(y).$$

The two loading conditions (5.2.30) are given by

$$\frac{W_i}{c} = \int_{s_i} dy' p(y') = \int_s dy L_i(y) w(y) + h_q \cos(\pi\theta) \int_{s_i} dy w(y), \quad i = 1, 2. \tag{6.1.39}$$

where

$$L_i(y) = \begin{pmatrix} L_{i1}(y) \\ L_{i2}(y) \end{pmatrix}, \quad y \in s_i, i = 1, 2,$$

$$L_{ij}(y) = \frac{h_q \sin(\pi\theta)}{\pi m_j(y)} \int_{s_i} dy' \frac{m_i(y')}{(y - y')}, y \in s_j, \; j = 1, 2.$$

6.1.2 Algebraic Equations for The Two-load case

Equation (6.1.9) may be reduced without difficulty to a set of algebraic equations. We rewrite it in a vector form:

$$v(y) = \begin{pmatrix} v_1(y) \\ v_2(y) \end{pmatrix} = \begin{pmatrix} e^{-\alpha(y-a_1)}(\int_{s_1} dy' \hat{K}_{11} v_1 + \int_{s_2} dy' \hat{K}_{12} v_2) \\ e^{-\alpha(y-a_2)}(\int_{s_1} dy' \hat{K}_{21} v_1 + \int_{s_2} dy' \hat{K}_{22} v_2) \end{pmatrix} + \begin{pmatrix} I_1(y) \\ I_2(y) \end{pmatrix}. \tag{6.1.40}$$

If the indentor profiles are given by the polynomials

$$f_i(y) = \sum_{r=0}^{m_i} d_{ir} y^r, \quad i = 1, 2,$$

the inhomogeneous terms $I_1(y), I_2(y)$ in equation (6.1.40) have the forms from equations (6.1.30) and (6.1.31),

$$I_i(y) = e_{i0} e^{-\alpha(y-a_i)} + \sum_{r=0}^{m_i} q_{ir} y^r, \quad i = 1, 2, \tag{6.1.41}$$

which are obtained by integrating (6.1.30) and (6.1.31) by parts. The quantities e_{i0} and q_{i0} are known explicitly apart from the fact that they depend on the contact intervals. For the indentor profiles given by (6.1.33), which are mainly of interest, we obtain

$$e_{10} = \frac{l_1 C}{\alpha R_1}(\ 1 + a_1 - \frac{1}{\alpha}) = -(\bar{h}G_0)\frac{G_1 C}{G_0 R_1}(\ 1 + a_1 - \frac{1}{\alpha}),$$

$$e_{20} = \frac{l_1 C}{\alpha R_2}(-1 + a_2 - \frac{1}{\alpha}) + \frac{l_1 C}{\alpha R_1} I_{120}$$

$$= -(\bar{h}G_0)[\frac{G_1 C}{G_0 R_2}(-1 + a_2 - \frac{1}{\alpha}) + \frac{G_1 C}{G_0 R_1} I_{120}],$$

$$q_{11} = \frac{C}{R_1}(-l_0 - \frac{l_1}{\alpha}) = -(\bar{h}G_0)\frac{C}{R_1},$$

$$q_{10} = \frac{C}{R_1}(-l_0 - \frac{l_1}{\alpha} + \frac{l_1}{\alpha^2}) = -(\bar{h}G_0)[\frac{C}{R_1}(1 + \frac{G_1}{G_0\alpha})],$$

$$q_{21} = \frac{C}{R_2}(-l_0 - \frac{l_1}{\alpha}) = -(\bar{h}G_0)\frac{C}{R_2},$$

$$q_{20} = \frac{C}{R_2}(\ l_0 + \frac{l_1}{\alpha} + \frac{l_1}{\alpha^2}) = (\bar{h}G_0)[\frac{C}{R_2}(1 - \frac{G_1}{G_0\alpha})],$$

where

$$I_{120} = e^{-\beta(a_2 - b_1)}[(-1 + \frac{1}{\alpha} - b_1) + e^{-\alpha D_1}(\ 1 - \frac{1}{\alpha} + a_1)].$$

From (6.1.40) and (6.1.41), we have that $v(y)$ can be expressed as

$$\begin{pmatrix} v_1(y) \\ v_2(y) \end{pmatrix} = \begin{pmatrix} g_{10}e^{-\alpha(y-a_1)} + \sum_{r=0}^{m_1} q_{1r}y^r \\ g_{20}e^{-\alpha(y-a_2)} + \sum_{r=0}^{m_2} q_{2r}y^r \end{pmatrix} \tag{6.1.42}$$

Substituting equations (6.1.42) into (6.1.40) and comparing coefficients, we obtain

$$g_{10} = A_{11}g_{10} + A_{12}g_{20} + B_{10} \tag{6.1.43}$$

$$g_{20} = A_{21}g_{10} + A_{22}g_{20} + B_{20}, \tag{6.1.44}$$

where

$$A_{ij} = \int_{s_j} dy' \hat{K}_{ij}(y')e^{-\alpha(y' - A_j)}, \quad i,j = 1,2,$$

$$B_{i0} = \sum_{j=1}^{2} \int_{s_j} dy' \hat{K}_{ij}(y') \sum_{r=0}^{m_j} q_{jr}y^r + e_{i0}.$$

The constants A_{ij} and B_{i0} are related to the parameters A_i and B_i implicitly. Combining (6.1.43) and (6.1.44) with the constraint conditions, (6.1.37) and (6.1.39), we can determine the constants g_{10} and g_{20}, which give the function $v(y)$ and the parameters of the contact regions A_i and B_i. Then the pressure $p(y)$ and other quantities of interest can be determined.

6.2 Numerical Results

In this section, we present numerical solutions of the equations for the one indentor and the two indentor case. Detailed results are presented for two values of the parameter

$$C_v = G_1/G_0. \tag{6.2.1}$$

The computation was performed on the SUN Computer Network in the Department of Mathematics & Statistics, at Simon Fraser University, supported by various powerful software packages including Fortran 77, S-plus, Gnuplot, Latex, Fig2 and Matlab.

6.2.1 Results for The One-indentor Case

Figure (5.1) gives a schematic diagram of the contact geometry for a moving rigid indentor on a lubricated viscoelastic half plane. A uniform load W per unit length is acting on the indentor. The indentor is assumed to move at sufficiently low speed V in the negative direction of x-axis, so that inertial effects can be neglected. The indentor axis is displaced backward from the contact center, which is the origin of the dimensionless system. The semicontact width a_0 for zero velocity has the relation (6.1.34) with load W and radius R of the indentor. For the linear theory of elasticity to apply, a_0 must be small compared with R. In the computation the value of a_0/R is fixed as 0.05. The material mechanical response are assumed to be that of a standard linear solid, with a fixed value of Possion's ratio ν_0.

The one load case involves solving three implicit equations (5.1.10), (5.1.11) and (5.1.12) for d_1, d_0 and C_1. When these three quantities are obtained, the problem is solved completely. The quantity d_1 is related to the contact interval length $(b-a)$ while d_0 gives the shift $(b+a)/2$ away from the origin of the indentor tip and C_1 determines the quantity $v(x)$. The three implicit equations are solved here by an iteration method. All the corresponding results are similar to Hunter's [26]. Also they are same as that obtained directly by solving the integrals (5.1.5 - 5.1.7).

Figure (6.1) shows the position of the end points of the contact region a/a_0 and b/a_0 as functions of velocity, $(V\tau'/a_0)$, for $C_v = 1$, $C_v = 9$. Figure (6.2) gives d_0/a_0 and d_1/a_0 as functions of $(V\tau'/a_0)$ for $C_v = 1$ and $C_v = 9$. The results show that in the viscoelastic case, the length of contact region, $b-a$, always is smaller than $2a_0$, the length of the elastic

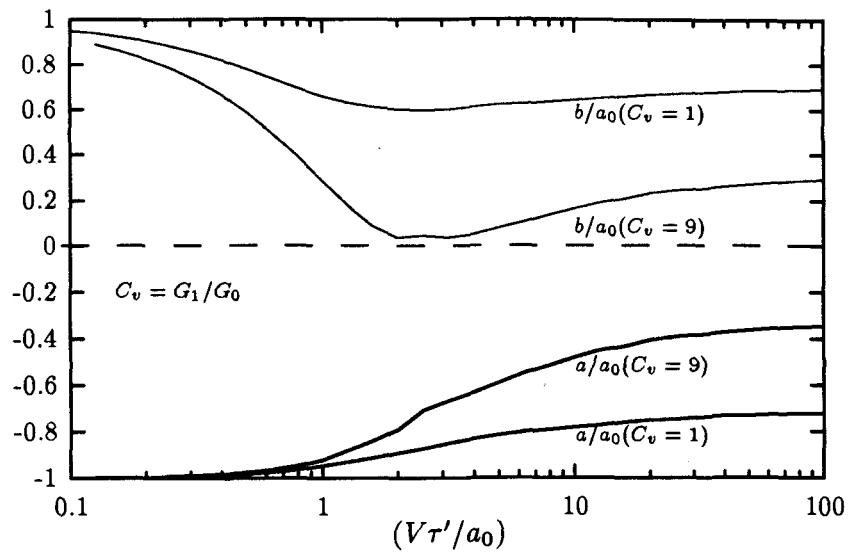

Figure 6.1: One indentor: variation of the values of a/a_0 and b/a_0 with velocity. The quantity a_0 is the semi-contact width for a cylinder in the elastic case, a and b are the end points of the contact region, while τ' is the decay parameter in the creep function.

contact region. The larger the value of C_v, the smaller the length. Also the contact region shifts toward the front. The variation of shift with velocity has a hump shape with velocity.

The corresponding plots for $f_H R/a_0$ are displayed in figure (6.3), where f_H is the coefficient of hysteretic friction discussed in section (4.1). The figures are similar to the shape of the shift of the tip. The pressure distribution is shown in figure (6.4) and figure (6.5) for the cases of $C_v = 1$ and $C_v = 9$ respectively, when $V\tau'/a_0 = 1.0$, which is roughly the value at which f_H is maximum. On each plot, we also display the Hertzian pressure distributions obtained for speeds $V = 0$ and $V = \infty$. All of these give relations identical to those of Hunter [26], allowing for the different convention for velocity direction.

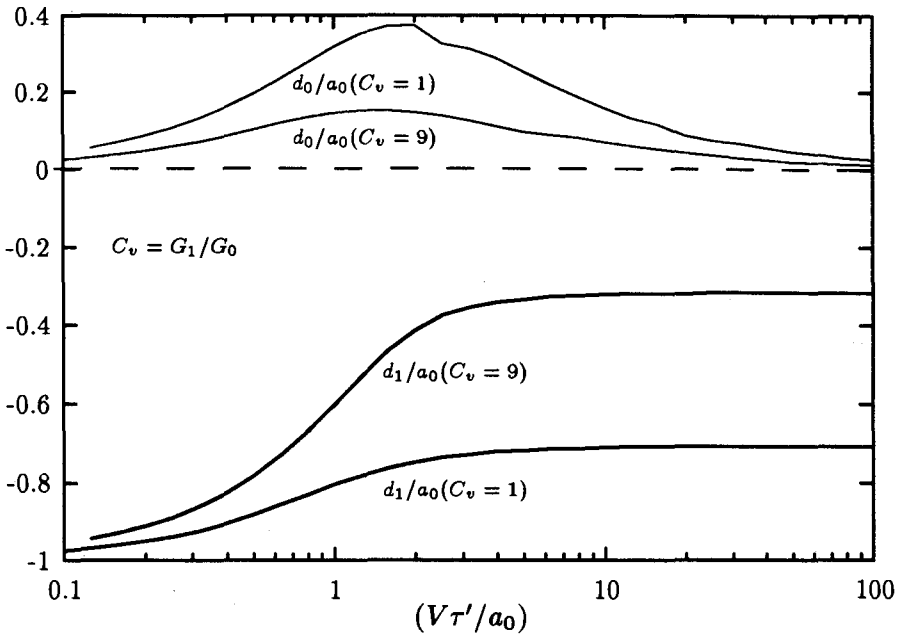

Figure 6.2: One indentor: variation of the shift of tip d_0 and contact interval quantity d_1 with velocity.

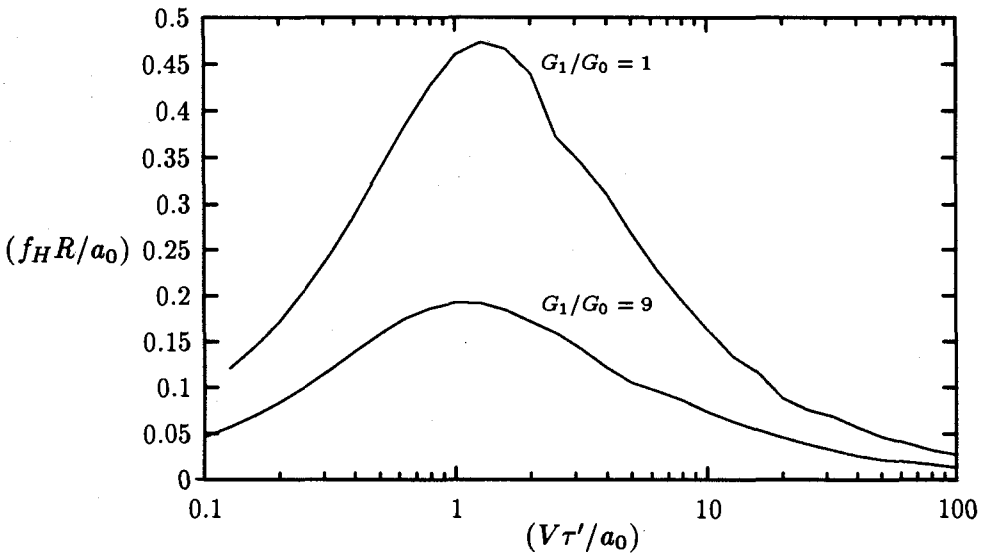

Figure 6.3: One indentor: variation of coefficient of hysteretic friction with velocity.

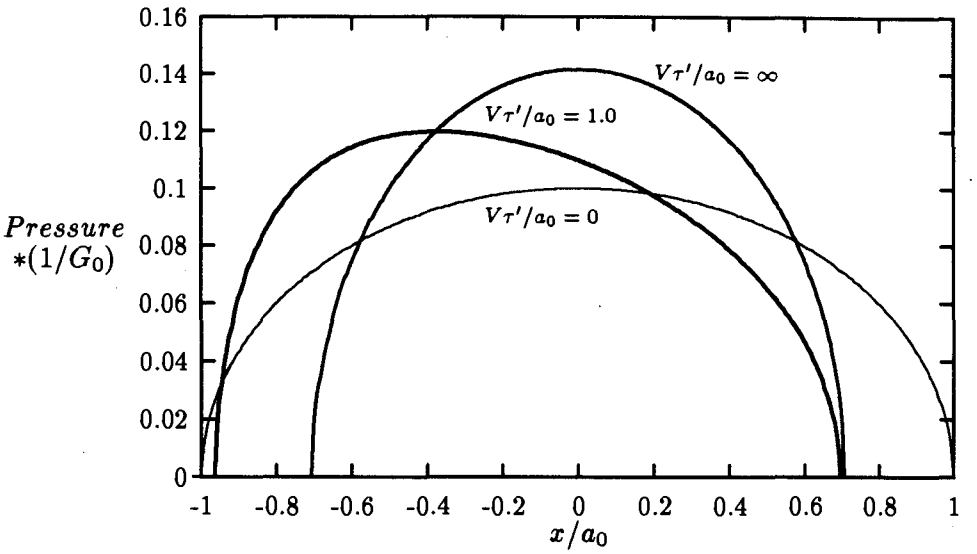

Figure 6.4: One indentor: pressure distribution over the contact region, $C_v = 1$.

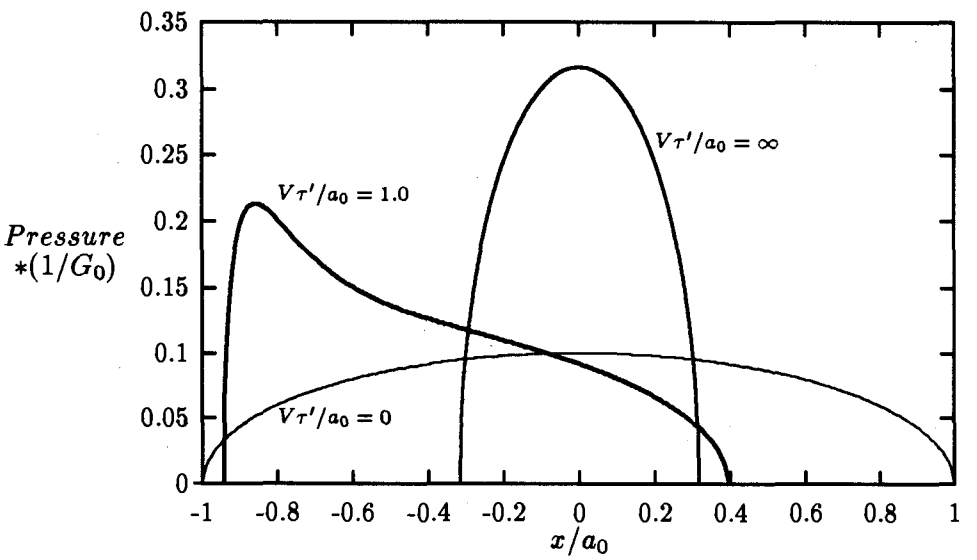

Figure 6.5: One indentor: pressure distribution over the contact region, $C_v = 9$.

6.2.2 The Two-indentor Case: Iteration

For the two-load case, whose cross section is shown in figure (5.2), integral equation (6.1.9) for $v(y)$, could not be simplified in terms of the modified Bessel functions with imaginary argument as in the single load case [19, 26]. The kernels $K_{ij}(y, y')$ given by equations (6.1.21 - 6.1.24) must be evaluated numerically. There are integrable singularities in the kernels $K_{ij}(y, y')$ and in the integrals of both solvability conditions (6.1.37) and load conditions (6.1.39) as well. The appropriate quadrature formula, either the mid-point rule or the left-end-point rule or the right-end-point rule, was chosen depending on where the singularities were. The goal of such a choice was to ensure that integrands were not evaluated at $y = y'$ points or the end of the contact regions, so that integrable singularities occurring at such points were avoided.

A complication, arising in the moving indentation problem, is that the extent of the contact regions is unknown a priori. Integral equation (6.1.9) and the subsidiary conditions, (6.1.37) and (6.1.39), determine implicitly the function $v(y)$ and the end points A_j and B_j of the contact regions. This system must be solved iteratively by numerical methods.

The iteration scheme proposed here may be described as follows. Make some initial guess at the values of A_j and B_j, $j = 1, 2$. The quantities K_{ij} and I_j are then determined by equations (6.1.21 - 6.1.24) and (6.1.30,6.1.31). The results are substituted in (6.1.9), to obtain $v(y)$.We refer to these as $\{A_j^{(0)}, B_j^{(0)}, v^{(0)}(y)\}$. Applying the two-load conditions, (6.1.39), we adjust the lengths of each interval D_i respectively. The shifts of the front end points, δA_j, are determined by using solvability conditions (5.2.28), and the new lengths, D_j. From the values of δA_j and D_j, we get a new set values of A_j and B_j, which we take as the next approximation. The iteration procedure may be repeated to the desired level of accuracy. We need to make a good guess at the initial values of A_j and B_j, so that the iteration converges sufficiently rapidly. In particular, a natural starting point is to take each contact region for the single-indentor problem, and use the results given in the last section. The assumptions for the one-indentor case are assumed to hold for the two-indentor case here, such as low speed, small deformation and material properties.

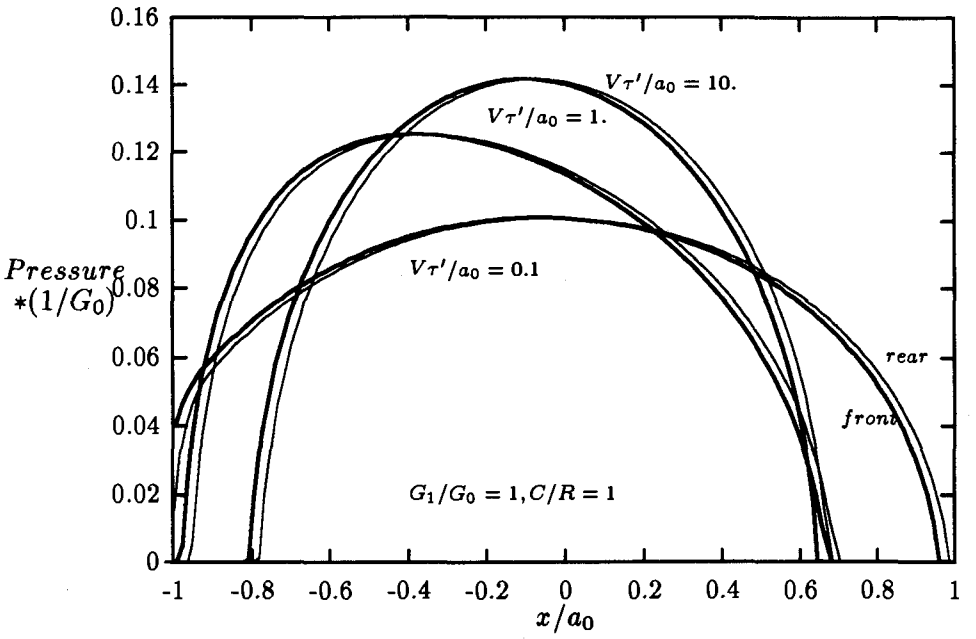

Figure 6.6: The two-indentor case: Pressure distributions over the contact regions. For comparison, the two contact regions are plotted together with the deepest points, $\bar{x}_{01}$ and $\bar{x}_{02}$, coinciding at $x = 0$. In this figure $C/R = 1$, $C_v = 1$.

6.2.3 The Two-indentor Case: Pressures

In the two-indentor case, the contact geometry is described by two sets of data $\{a, b, R, W\}$, one for each indentor, and the distance $2C$ between the two indentor axes (figure (5.2)). In the numerical results represented here, the ratios of static semicontact width to radius (a_0/R) of both indentors are fixed as 0.05. Each supporting load W_i depends on each radius in the manner indicated by (6.1.34).

Taking both radii to be equal, $R_1 = R_2$, we show the pressure distributions under both indentors in figures (6.6, 6.7) for the case of $C_v = G_1/G_0 = 1$. For comparison, the two contact regions are plotted together with the deepest points $\bar{x}_{01}$ and $\bar{x}_{02}$ coinciding at $x = 0$ in the figures.

In each figure, three pairs of the pressure distributions are represented for $V\tau'/a_0 = 0.1, 1$, and 10. When compared with figure (6.4), the pressure of the one-load case, the numerical results in figures (6.6, 6.7) show that the solution obtained degenerates into the

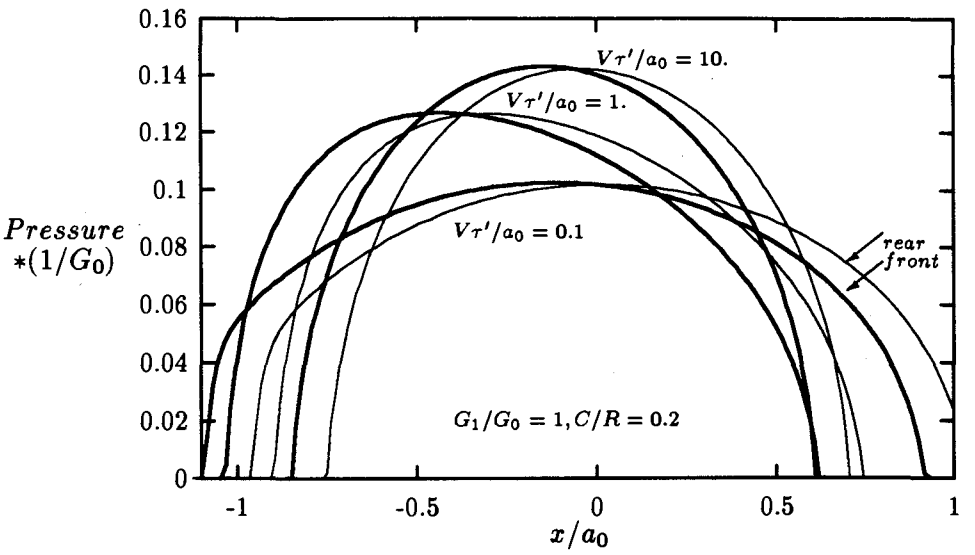

Figure 6.7: The two-indentor case: Pressure distributions, $C/R = 0.2$, $C_v = 1$.

appropriate elastic solution, the Hertzian pressure distribution in two ways as follows. First, for sufficiently large velocities, the pressure distributions are symmetric about $x = \bar{x}_{0j}$, the deepest points of the indentors. This is a reflection of the fact that the viscoelastic medium behaves in this limit as an elastic solid with shear modulus

$$G_d = G_0 + G_1, \tag{6.2.2}$$

which is the dynamic shear modulus. In this case, the contact interval length reduced to about $100/\sqrt{G_d/G_0}\%$ of $2a_0$. The maximum pressure increases to about $100\sqrt{G_d/G_0}\%$ of the maximum static pressure P_0, P_0 is related to the mean elastic pressure P_m [30] by

$$P_0 = \frac{2W}{\pi a_0} = \frac{4}{\pi} P_m, P_m = \frac{W}{2a_0},$$

$$P_0 = \sqrt{\frac{WG_0}{\pi R(1-\mu)}}.$$

Second, for sufficiently small velocities, the results again reduce to the elastic case but with G_d replaced by the 'static' modulus G_0, which is the shear modulus at the large time limit. We refer to G_0 as the elastic shear modulus. A similar argument applies in the one-load case [26].

Also, the results in figures (6.6, 6.7) illustrate a phenomenon that the pressure distributions under the front indentor are always to the left of those under the rear indentor. In other words, the contact area of the front one is shifted a little more than that of the rear one, along the direction of motion. As C/R reduces, which means that the two indentors are close each other, there is a more pronounced difference between the shapes of the pressure distribution under each indentor.

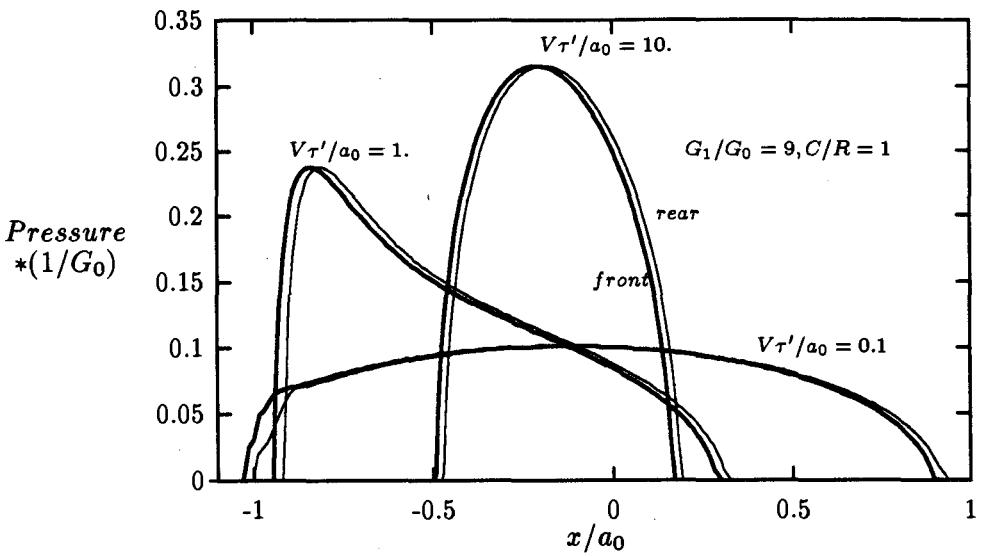

Figure 6.8: The two-indentor case: Pressure distributions, $C/R = 1$, $C_v = 9$.

For the case, $C_v = G_1/G_0 = 9$, the pressure distributions under both indentors are shown in figures (6.8, 6.9). The results for the single-indentor case are shown on figure (6.5).

Figures (6.10, 6.11) show the variation of the positions of the end points of the contact regions with velocity. Also they give the results of the elastic case and the one-load case for comparison. The two indentors have the same sizes and $C/R = 0.2$. The curves will presumably be asymptotic to the straight lines with the modulus G_0+G_1 or G_0, which are the elastic limits. Figure (6.12) shows the variation of the shifts and the half-lengths of contact regions with velocity, where the shifts are $d_{01} = (b_1 + a_1 + 2)/2$ and $d_{02} = (b_2 + a_2 + 2)/2$, and the half-lengths are $-d_{1i} = (b_i - a_i)/2$, $i = 1, 2$. The lengths of each contact region

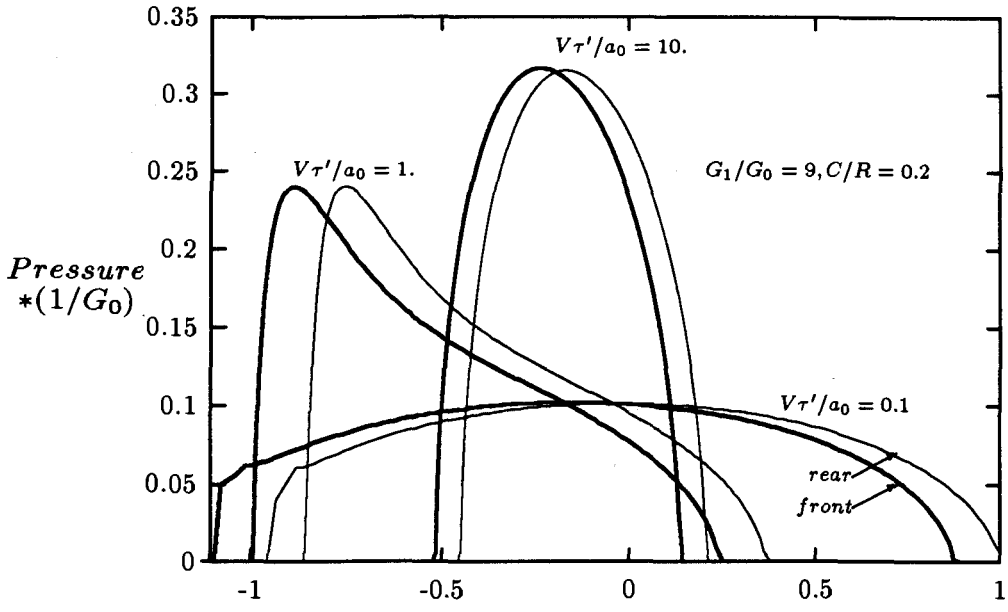

Figure 6.9: The two-indentor case: Pressure distributions, $C/R = 0.2$, $C_v = 9$.

are little different from each other, and are almost same as the one-load case. Comparing with the shifts in the elastic case, that of the front one is forward $0.065a_0$ and that of the rear one is backward $0.066a_0$. Both shifts have the same shape with respect to velocity, and when the velocity is large, the difference between them reduces and they are close to that in the one-indentor case. It is also noted that for symmetric loading and symmetric indentor profiles, the contact regions are not symmetric.

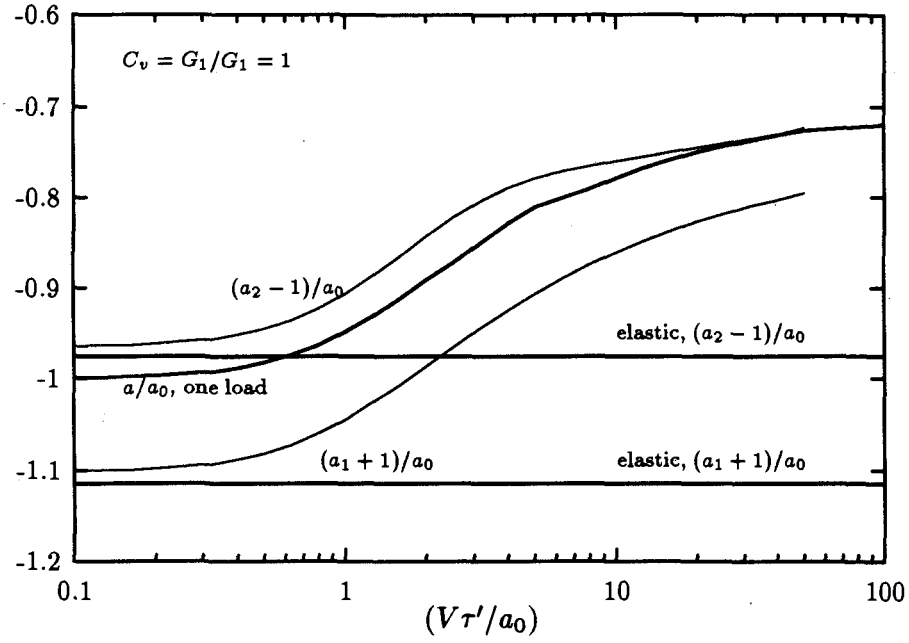

Figure 6.10: The two-indentor case: Variation of the positions of the front end points of contact regions with velocity, comparing with the elastic case which are straight lines. The quantities, a_1 and a_2, are the front end points of the front and rear indentors respectively in the dimensionless system. $C/R = 0.2$, $C_v = 1$.

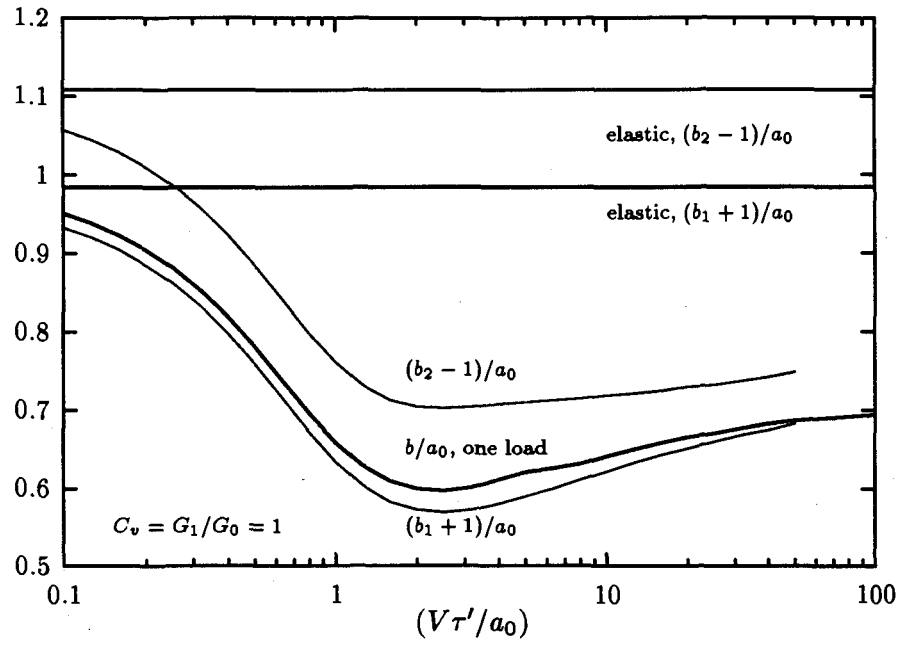

Figure 6.11: The two-indentor case: Variation of the positions of the rear end points of contact regions with velocity, comparing with the elastic case given by straight lines. $C/R = 0.2$, $C_v = 1$.

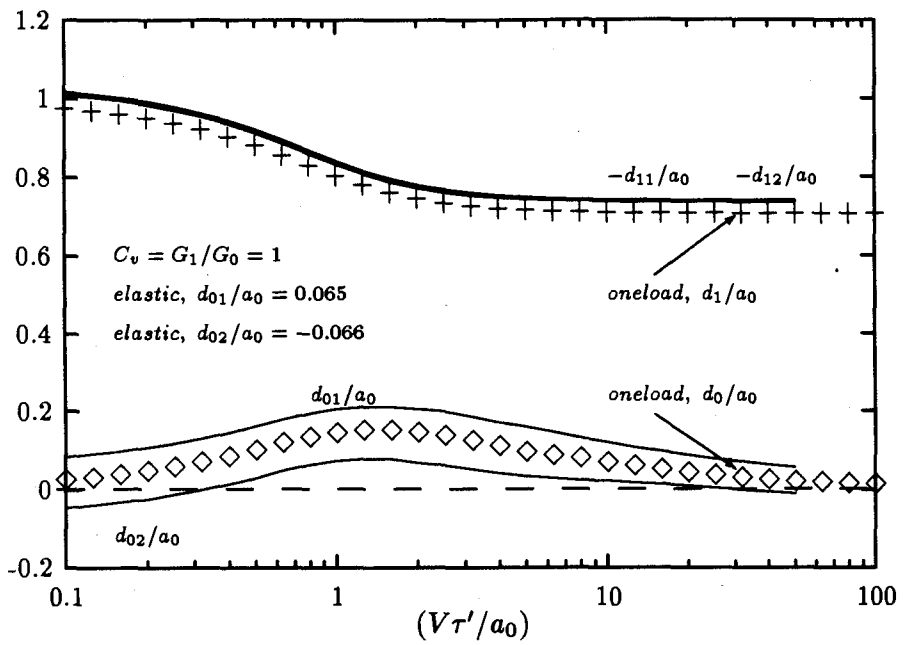

Figure 6.12: Variation of the shifts, d_{01} and d_{02}, and the half-lengths, $-d_{11}$ and $-d_{12}$, of the contact regions with velocity, compared with the elastic case which are straight lines. $C/R = 0.2$, $C_v = 1$.

6.2.4 The Two-indentor Case: Hysteretic Friction

We now give the results for the coefficient of hysteretic friction [14, 18, 19, 24, 39]. Equation (4.2.7), adapted to a dimensionless system for two cylindrical indentors, yields a coefficient of hysteretic friction which in the stationary coordinate system has a general form:

$$f_H = \frac{C}{W}\int_s dx p(x) f(x) \tag{6.2.3}$$

where $p(x)$ is the pressure distribution in the contact regions while the function $f(x)$ is the derivative of the indentor profiles given by (3.2.1), and s represents the stationary contact regions given by equation (6.1.5). Also

$$W = W_1 + W_2 \tag{6.2.4}$$

is the total load. Functions (6.1.33) for $f(x)$ are used in this two-indentor case.

For each indentor, the tangential force coefficient has the form

$$f_{H_j} = \frac{C}{W_j}\int_{s_j} dx p(x) f_j(x). \tag{6.2.5}$$

General form (6.2.3) shows that f_H is a weight average obtained by summing the individual f_{H_i}, weighted with respect to loads:

$$f_H = \sum_{j=1}^{2} \frac{W_j}{W} f_{H_j}. \tag{6.2.6}$$

Each of the moving indentors considered here has an axis of symmetry, and the distance, $2C$, between these two indentors does not change. Equation (6.2.3) shows that the fundamental reason for hysteretic friction on a well lubricated surface is caused by deformation and recovery under the indentor or indentors. The deformation and recovery are not symmetrical with respect to each axis of symmetry in the viscoelastic case. In fact the asymmetry happens in the elastic case too, since the deformation on the surface between two indentors is much larger than that on the outer parts of the surface. In general, a non-zero tangential force acts on each indentor. However, on the whole system, the total tangential force must be zero as the total loss of energy is zero.

This is easily demonstrated in the case of two indentors which have same size and sharpe. As the loading, material and pressure distribution are symmetrical about $x = 0$, and the

function $f(x)$ is an odd one, f_H evaluated by (6.2.3) vanishes. Hysteretic friction is a viscoelastic effect.

In general, in the elastic case, when the indentors are in motion, the force under the front one resists the motion, and the rear one exerts the same magnitude of the force, but in the opposite direction. The forces must cancel each other. We may refer to the force under the front indentor as F_{e1}, the force under the rear indentor as F_{e2}.

$$F_{e1} = f_{e1}W_1, \qquad F_{e2} = f_{e2}W_2, \tag{6.2.7}$$

where f_{ej}, $j = 1, 2$ are the coefficients of the elastic tangential forces under each indentor. In the two-indentor case, $F_{e1} + F_{e2} = 0$. Such forces will effect the tangential force under the individual indentor. Using formula (6.2.5) for the tangential force coefficient of an individual indentor, we see that it affected by both the viscous and F_{ej} forces. The magnitude of the effect of elastic deformation, f_{ej}, can be computed by a formula similar to equation (6.2.5). The solution for the elastic case can be obtained by setting $C_v = 0$ or by solving multi-indentor equations [6] in elasticity.

Table (6.1) gives the values of f_{e1} compared with f_H for four different cases. In each case, the two indentors have the same size and same loading, but the distance between them is different from the other cases. The results show that the closer the indentors, the larger f_{e1} becomes. Also the table gives the maximum values of the coefficient of hysteretic friction for the system, which we can take as the weighted average value mentioned above. Compared with the quantity, f_H, when $C_v = G_1/G_0 = 1$, the effect of f_{ej} can be ignored when $C/R > 1$. If $C/R > 1$ then a_0/C is less than 5% in our computation as the ratio C/R is inversely proportional to a_0/C, the ratio of the static semicontact width to the half distance between the two indentors, and a_0/R is equal to 0.05. The effect of f_{ej} has same order of the magnitude as that of hysteretic when a_0/C is close to 0.5 ($C/R \sim 0.1$). For $C_v = 9$, the viscous effect is about two and half times of that for $C_v = 1$. Note that the quantity f_H is not proportional to the coefficient C_v.

	$C/R = 5.0$	$C/R = 1.0$	$C/R = 0.2$	$C/R = 0.1$
f_{e1}, $C_v = 0$	0.00252	0.0129	0.0660	0.148
f_H, $C_v = 1$	0.198	0.206	0.201	0.196
f_H, $C_v = 9$	0.481	0.498	0.482	0.470

Table 6.1: Comparison of the elastic tangential force under each indentor with the hysteretic friction force for different distances between the two indentors. f_{e1} is the coefficient of the elastic tangential force under the front indentor. f_H is the coefficient of hysteretic friction for the two-indentor system. $C_v = G_1/G_0$, $a_0/R = 0.05$

The region of velocity in which f_{H2} takes negative sign		
C/R	$V\tau'/a_0$ Less than	$V\tau'/a_0$ Greater than
0.10	0.32	10.0
0.15	0.24	20.0
0.20	0.13	32.0
1.00	0.1	100.

Table 6.2: The region of dimensionless velocity $V\tau'/a_0$ in which the sign of the tangential force under the rear indentor is negative.

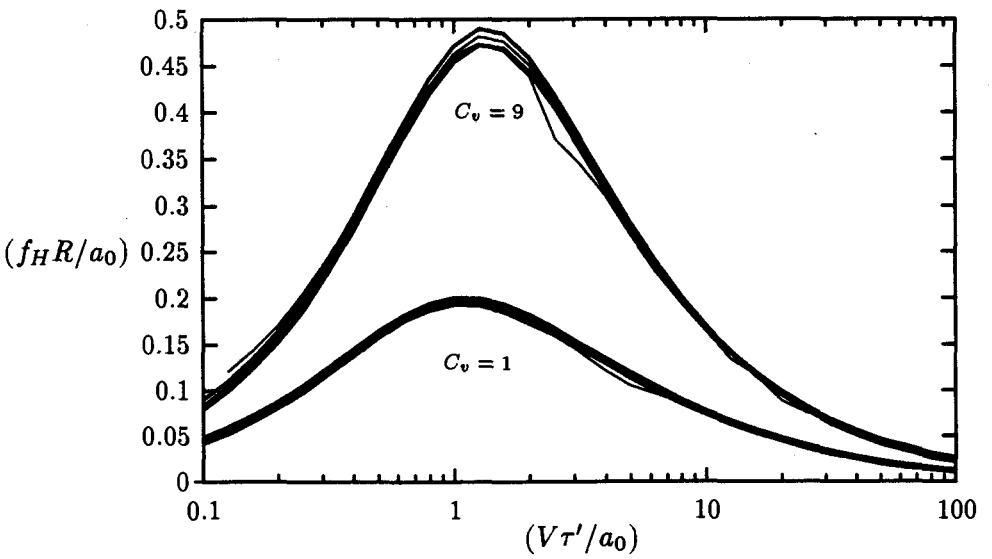

Figure 6.13: The two-indentor case: Variation of the coefficient of hysteretic friction with velocity, $C/R = 5$, $C_v = 1$ and 9.

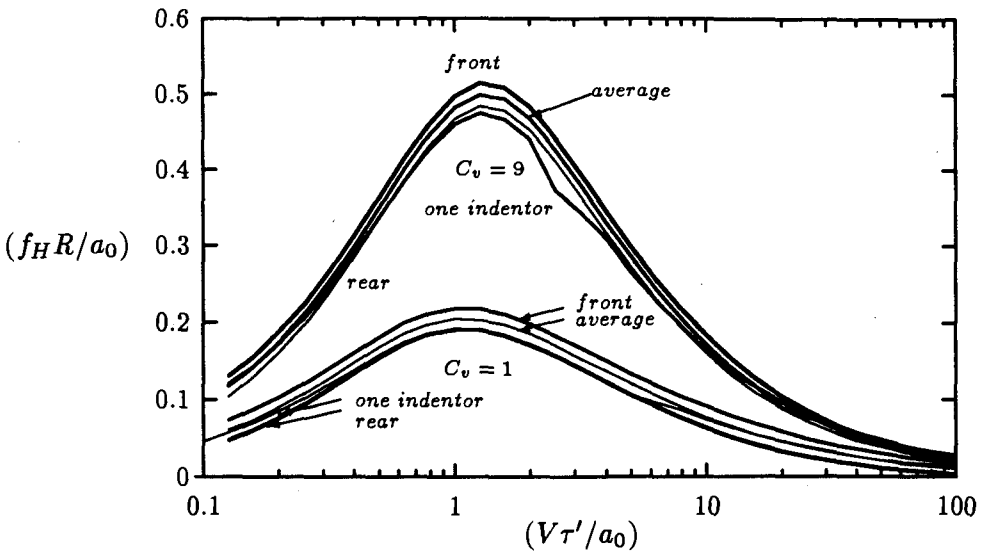

Figure 6.14: The two-indentor case: Variation of the coefficient of hysteretic friction with velocity, $C/R = 1$, $C_v = 1$ and 9.

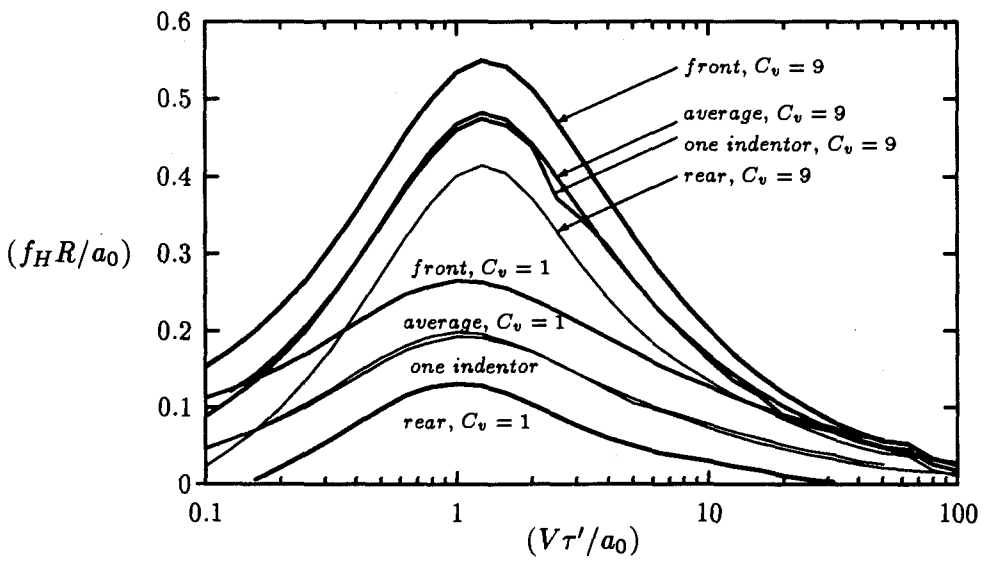

Figure 6.15: The two-indentors case: Variation of the coefficient of hysteretic friction with velocity, $C/R = 0.2$, $C_v = 1$ and 9.

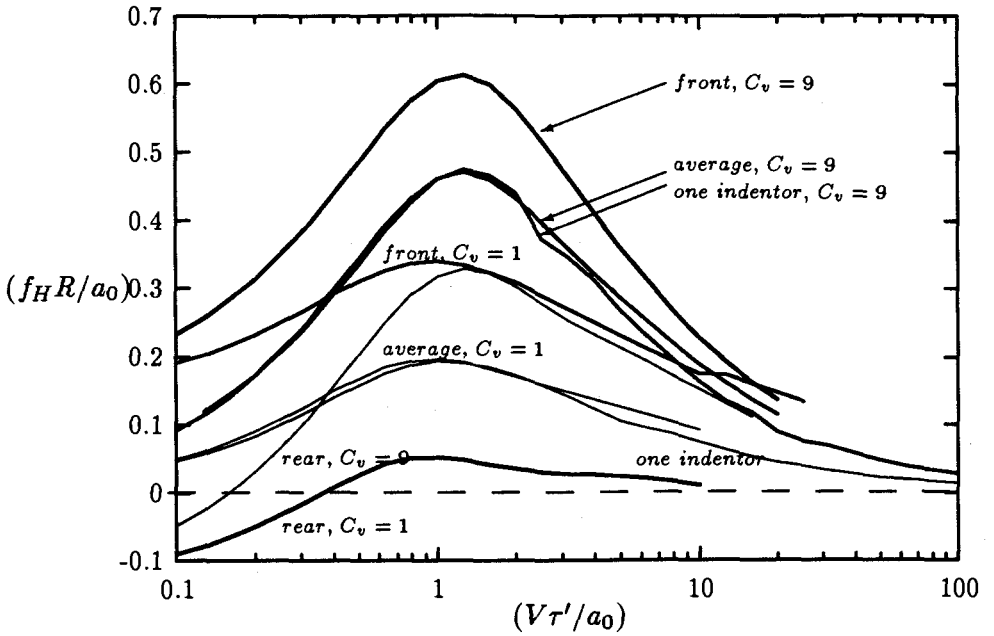

Figure 6.16: The two-indentor case: Variation of the coefficient of hysteretic friction with velocity, $C/R = 0.1$, $C_v = 1$ and 9.

Intuitively, we can see that on a lightly viscoelastic material with moving indentors, the resistance to the motion of the front indentor will increase and the forward force on the rear indentor will diminish. The latter passes through zero for a certain level of viscoelastic loss which will depend on the separation of the indentors. As viscous effects increase further, both indentors experience resisting forces, although that on the rear indentor is less than that on the front indentor. For any level of viscoelasticity, the sum of the forces is non-zero and in a direction opposing the motion. This sum will contain no effect of asymmetrical deformation and depends upon hysteretic phenomena only.

This intuitive prediction is supported by the numerical results shown in figure (6.13 ~ 6.15) and table (6.1). In figure (6.17), f_{e2} is compared with f_{H1}, f_{H2} and f_H.

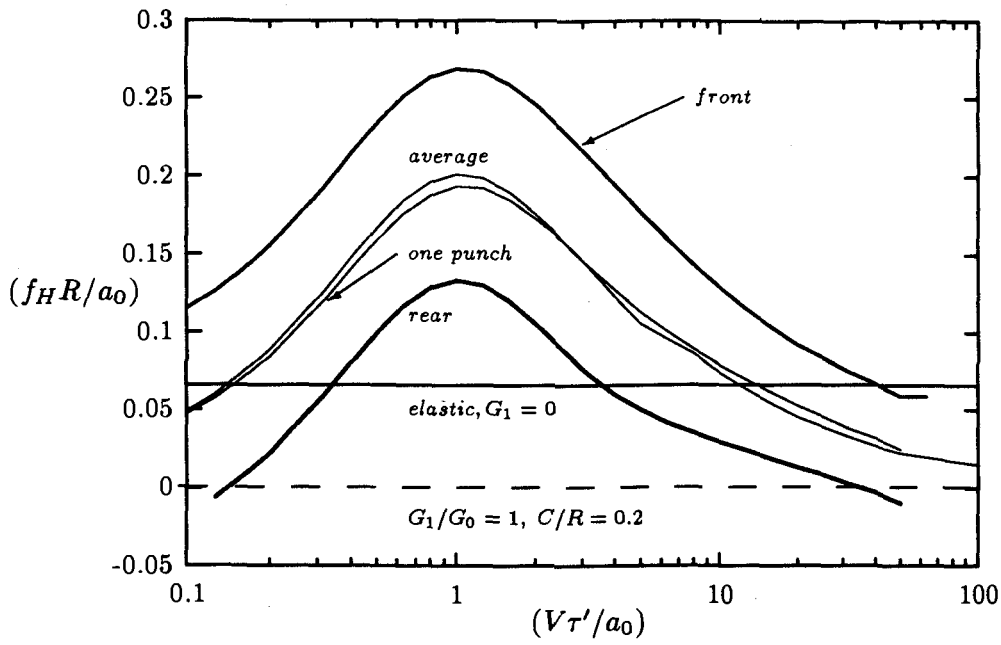

Figure 6.17: The two-indentor case: Hysteretic friction force compared with the tangential force under front indentor in the elastic case, $C/R = 0.2$, $C_v = 1$.

Figures (6.13), (6.14), (6.15), and (6.16) give the coefficient of hysteretic friction as a function of $(V\tau'/a_0)$. Each one presents f_{H_j}, the average value f_H, and the result for a single indentor. These are for two materials $C_v = 1$ and $C_v = 9$. Four values, $C/R =$ 0.1,0.2,1.0, and 5.0, are used in each case respectively. The tangential force under the rear indentor is not always negative as in the elastic case. It takes a negative value only when the two contact regions are close and velocity is small or large (see table (6.2)).

Table (6.3) gives the relative percentage difference of f_{H1} and f_{H2} which relates to the tangential forces under each indentor:

$$\delta_r = \frac{|f_{H1} - f_{H2}|}{f_{H1}} * 100, \tag{6.2.8}$$

where f_{H1} and f_{H2} take their maximum values. For a material characterized by C_v, the closer the indentors, the greater the difference between the two values of the tangential force coefficients. As the distance between the two indentors increases, the effect reduces. When $C/R > 5$, the two indentors can be considered as two single indentors moving independently. Each indentor experiences the same tangential force. The interference effect between the

	$C/R = 5.0$	$C/R = 1.0$	$C/R = 0.2$
$G_1/G_0 = 1$	4.17	13.95	78.57
$G_1/G_0 = 9$	4.08	7.45	23.91

Table 6.3: The relative percentage difference of f_{Hj} for two indentors when they take their maximum values.

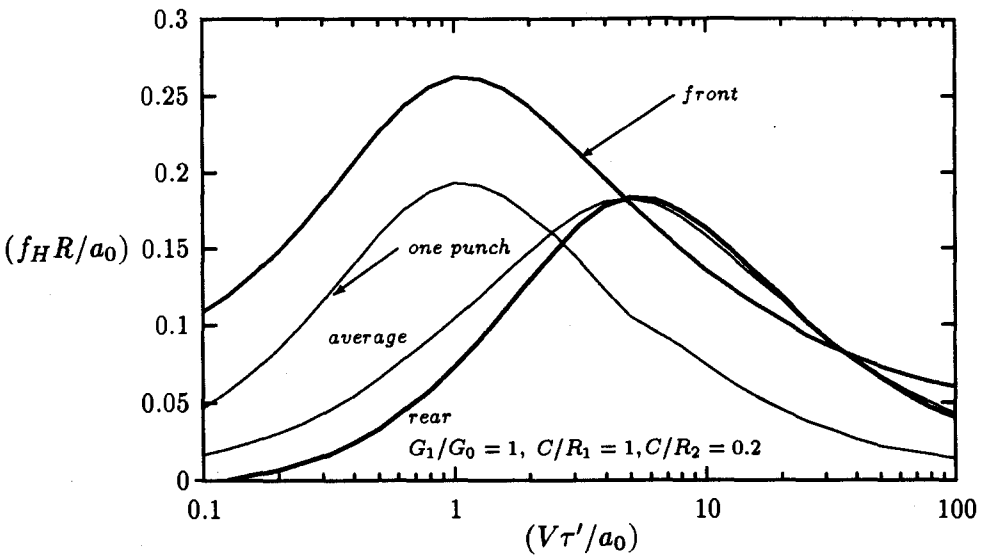

Figure 6.18: The two-indentor case: Variation of the coefficient of hysteretic friction with velocity. The size of the front indentor is smaller than the rear one. $C/R_1 = 1.0, C/R_2 = 0.2$, and $C_v = 1$.

indentors is negligible.

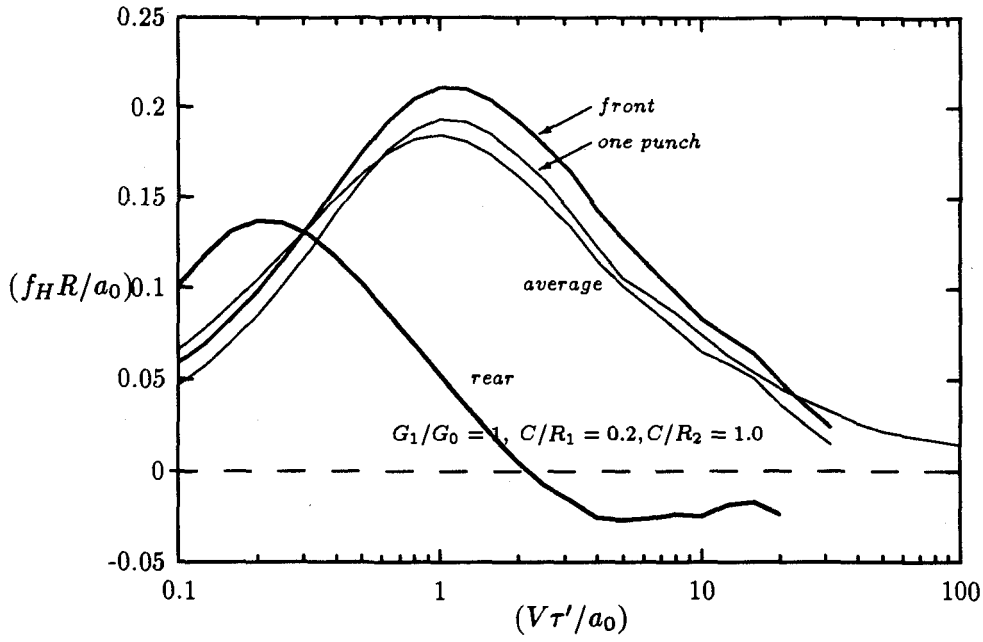

Figure 6.19: The two-indentor case: Variation of the coefficient of hysteretic friction with velocity. The size of the rear indentor is smaller than the front one. $C/R_1 = 0.2, C/R_2 = 1.0$, $C_v = 1$. Only if the velocity is large, will the friction under the rear indentor be negative.

Figures (6.18, 6.19) show the results for the two-indentor case in which the sizes of the two indentors are not the same. When the smaller indentor is at the rear, the hysteretic friction shape moves forward to the direction the velocity increases in the figure. When velocity is low, it is smaller than that in one-indentor case. If $V\tau'/a_0$ is greater than 2, it is great than that in the one-indentor case. Conversely, when the smaller indentor is in the front, the hysteretic friction does not change too much. But we find that if the velocity is large enough, the friction under the rear indentor will be negative. If $V\tau'/a_0$ is greater than 20 or so, the computation is not stable.

These results for the coefficient of hysteretic friction also indicate that the hysteretic friction for the two-indentor case as a function of speed has, roughly speaking, the hump shape observed experimentally. It reaches the maximum value when the velocity is of order a_0/τ'. For the four cases we chose, in each of which the sizes of two indentors are same, the function is very close to the f_H curve of the one-indentor case. Also, it approaches zero for sufficiently small and large values of velocity. The later observation corresponds to the fact

that the pressure distribution tends to be symmetric form for $V \to 0$ or $V \to \infty$, which are the two elastic limits mentioned above.

Figure (6.20) shows the results of the stress σ_{22} distribution in the material, $y > 0$. This is an example which shows that quantities of interest can easily be obtained after the quantity $v(x)$ and the contact intervals are known. When $y = 0$, figure (6.20) illustrates the pressure distribution along the boundary.

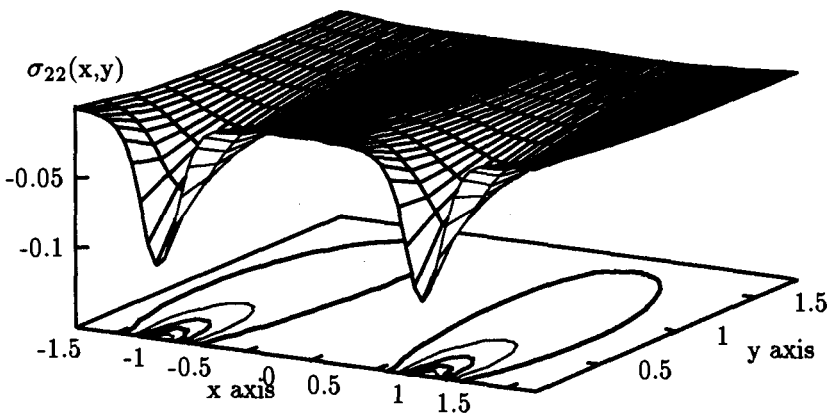

Figure 6.20: The stress σ_{22} distribution in the material, $y > 0$. When $y = 0$, this distribution illustrates the pressure on the contact regions. $C_v = 9$, $C/R = 0.2$.

6.3 Summary and Further Work

The problem of two or more indentors moving over the surface of a viscoelastic plane is considered. The solution of this mixed boundary value problem with moving boundaries is formulated in terms of a coupled system of integral equations in space and time. The decomposition of hereditary integrals plays an important role in the derivation. These formulae are applicable to the general linear viscoelastic material.

Equations for the two-indentor case are given in detail. For the standard linear solid and steady-state conditions, such equations form to a set of non-linear algebraic equations, which contain singular integrals on the unknown moving regions. Numerical results are obtained and analyzed qualitatively for two values of the viscous parameter, different distances between the two indentors, and different sizes of each indentor. The phenomena of hysteretic friction and the interaction between the two indentors are explored. The latter one is compared with the elastic results which may be taken as a special case of the more general formulation.

Further work would include the case of an infinite number of indentors. In this case, the pressure at infinity is not zero. The effect of inertia could be also studied. As the superposition principle is not applicable in this kind of moving contact problem, moving indentation problems under varying loads also would be interesting.

Bibliography

[1] Bapat, C.N. and Batra, R.C., Finite Plane Strain Deformations of Nonlinear Viscoelastic Rubber-covered Rolls, *International Journal for Numerical Methods in Engineering*, Vol. 20, pp. 1911-1927, 1984.

[2] Boltzmann, L., *Wissenschaftliche Abhandlungen*, Vol. 1, P. 167 of his Collected Papers (1909), reprinted by Chelsea, New York, 1968.

[3] Delves, L.M. and Mohamed, J.L., *Computational Methods for Integral Equations*, Cambridge University Press, 1985.

[4] Fichera, G., Problemi Elastostatici con Vincoli Unilaterale: il Probleme di Signorini con Anbigue Condizioni al Contorno, *Memorie Accademie Nazionale Dei Lincei*, Ser. 8,7, pp. 91-140, 1964.

[5] Ferry, John D., *Viscoelastic Properties of Polymers*, John Wiley & Sons, Inc., New York, 1970.

[6] Gladwell, G.M.L., *Contact Problems in the Classical Theory of Elasticity* SIJTHOFF & NOORDHOFF, 1980.

[7] Galin, L.A., *Contact Problems in the Theory of Elasticity*, Edited by I.N. Sneddon, Department of Mathematics, North Carolina State College, Raleigh, 1961.

[8] Galin, L.A., *Contact Problem in the Classical Theory of Elasticity and Viscoelasticity*, (In Russian). Izdatelstvo "Nauka", Moscow.

[9] Golberg, Michael A., *Numerical Solution of Integral Equation*, Plenum Press, 1990.

[10] Golberg, Michael A., *Solution Methods for Integral Equations*, Plenum Press, 1979.

[11] Golden, J.M. and Graham, G.A.C., A Proposed Method of Measuring the Complex Modulus of a Thick Viscoelastic Layer, *Rheologica Acta* Vol. 28(5), pp. 414-416, 1989.

[12] Golden, J.M., and Graham, G.A.C., The Transient Quasi-static Plane Viscoelastic moving Load Problem, *International Journal of Engineering Science* Vol. 25(1), pp. 65-84, 1987.

[13] Golden, J.M. and Graham, G.A.C., The Steady-state Plane Normal Viscoelastic Contact Problem, *International Journal of Engineering Science*, Vol. 25, pp. 277-291, 1987.

[14] Golden, J.M., Frictional Viscoelastic Contact Problems, *Quarterly Journal of Mechanics and Applied Mathematics*, Vol. 39(1), pp. 125-137, 1986.

[15] Golden, J.M., Approximate Analytic Treatment of the Problem of a Moving Ellipsoidal Punch on a Viscoelastic Half-space, *Quarterly Journal of Mechanics and Applied Mathematics*, Vol. 35(1), 1982.

[16] Golden, J.M., Hysteresis and Lubricated Rubber Friction, *Wear*, Vol. 65(1), pp. 75-87, 1980.

[17] Golden, J.M., The Problem of a Moving Rigid Punch on an Unlubricated Viscoelastic Half-plane, *Quarterly Journal of Mechanics and Applied Mathematics* Vol. 32(1), 1979.

[18] Golden, J.M., Hysteretic Friction of a Plane Punch on a Half-plane with Arbitrary viscoelastic Behaviour, *Quarterly Journal of Mechanics and Applied Mathematics*, Vol. 30(1), pp. 23-49, 1977.

[19] Golden, J.M. and Graham, G.A.C., *Boundary Value Problems in Linear Viscoelasticity*, Spring-Verlag, Berlin, Heidelberg, 1988.

[20] Graham, G.A.C. and Golden, J.M., The Generalized Partial Correspondence Principle in Linear Viscoelasticity, *Quarterly of Applied Mathematics*, Vol. 46(3), pp. 527-538, 1988; Vol. 49(2), p 379, 1991.

[21] Graham, G.A.C. and Sabin, G.C.W., The Correspondence Principle of Linear Viscoelasticity for Problems that Involve Time-dependent Regions, *International Joural of Engineering Science*, Vol. 11, pp. 123-140, 1973.

[22] Graham, G.A.C., The Contact Problem in the Linear Theory of Viscoelasticity where the Time Dependent Contact Area has any Number of Maxima and Minima, *International Joural of Engineering Science*, Vol. 5, pp. 495-514, 1967.

[23] Green, A.E. and Zerna, W. *Theoretical Elasticity*, the Clarendon Press, Oxford England, 1968

[24] Greenwood, J.A. and Tabor, D. Hysteresis Losses in Rolling and Sliding Friction, *Proceedings of the Royal Society (London)*, Vol. 259(A), pp. 180-507, 1961.

[25] Hertz, H., On the Contact of elastic Solids, *Miscellaneous Papers by H. Hertz*, English translation, Eds. Jones and Schott, London:Macmillan, 1896.

[26] Hunter, S.C., The Rolling Contact of a Rigid Cylinder with a Viscoelastic Half-space, *Journal of Applied Mechanics*, Vol. 28, pp. 611-617, 1961.

[27] Hunter, S.C., Viscoelastic Wave, *Progress in Solid Mechanics*, (editors: I.N. Sneddon and R. Hill), pp. 1-57, John Wiley & Sons, Inc., New York, 1964.

[28] Hunter, S.C., *Mechanics of Continuous Media*, Ellis Horwood, Chichester, 1976.

[29] Johnson, K.L., A Review of the Theory of Rolling Contact Stresses, *Wear*, Vol. 9, pp. 4-19, 1966.

[30] Johnson, K.L., *Contact Mechanics*, Combridge University Press, 1985.

[31] Kalker, J.J., *Three-dimensional Elastic Bodies in Rolling Contact*, Kluwer Academic Publishers, Netherlands, 1990.

[32] Lan, Q., Three-Dimensional Steady-state Normal Indentation Problem for a General Viscoelastic Material, *M.Sc. Thesis*, Simon Fraser University, 1991.

[33] Lee, E.H. and Radok, J.R.M., The Contact Problem for Viscoelastic bodies, *Journal of Applied Mechanics*, Vol. 27, pp. 438-444, 1960.

[34] Lodge, Arthnr S., *Body Tensor Fields in Continuum Mechanics*, Academic Press, New York, 1974.

[35] Maxwell, J.C., On the Dynamical Theory of Gases, (*Scientific Papers*, 1890), Vol. 2, pp. 26-78.

[36] Mclachlan, N.W., *Bessel Functions for Engineers*, Oxford at the Clarendon Press, 1955

[37] Morland, L.W., Rolling Contact between Dissimilar Viscoelastic Cylinders, *Quarterly of Applied Mathematics* Vol. 25, pp. 363-376, 1968.

[38] Morland, L.W., Exact Solutions for Rolling Contact between Viscoelastic Cylinders, *Quarterly Journal of Mechanics and Applied Mathematics*, Vol. 20(1), pp. 73-106, 1967.

[39] Morland, L.W., A Plane Problem of Rolling Contact in Linear Viscoelasticity Theory, *Journal of Applied Mechanics*, Vol. 29, pp. 345-352, 1962.

[40] Muskhelishvili, N.I., *Some Basic Problems of the Mathematical Theory of Elasicity*, P. Noordhoff Ltd.,Groninen, Translated from the Russian by J.R.M. Radok, 1963.

[41] Panek, C. and Kalker, J.J., 3-Dimensional Contact of a Rigid Roller Traversing a Viscoelastic Half-space, *Journal of the Institute Mathematics and Its Applications* Vol. 26, pp. 299-313, 1980.

[42] Porter, David and Stirling, David S.G., *Integral Equations*, Cambridge University Press, 1990.

[43] Sabin, G.C.W. and Kaloni P.N., Contact Problem of a Rigid Indentor with Rotational Friction in Second Order Elasticity, *International Journal of Engineering Science* Vol. 27(3), pp. 203-217, 1989.

[44] Shames, Irving H., *Mechanics of Deformable Solids*, Englewood Cliffs, New Jersey, 1964.

[45] Shames, Irving H. and Cozzarelli, Francis A., *Elastic and Inelastic Stress Analysis*, Prentice-Hall, Englewood Cliffs, New Jersey, 1992.

[46] Sneddon, I.N., *Fourier Transforms*, McGraw-Hill, New York, 1951.

[47] Sokolnikoff, I.S., *Mathematical Theory of Elasticity*, McGraw-Hill, New York, 1956.

[48] Tabor, D., The Importance of Hysteresis Losses in the Friction of Lubricated Rubber, *Proceedings of First International Skid Prevention Conference*, Part 1, Virginia Council of Highway Investigation and Research, Charlottesville, Virginia, 1957.

[49] Tabor, D., Mechanism of Rolling Friction, *Journal of Theoretical, Experimental and Applied Physics*, Vol.43(7), pp. 1055-1059, 1952.

[50] Timoshenko, S. and Goodier, J.N. *Theory of Elasticity*, McGraw-Hill, 1951.

[51] Ting, T.C.T., A Mixed Boundary Value Problem in Viscoelasticity with Time-Dependent Boundary Regions, in *Proceeding of the Eleventh Midwestern Mechanics Conference*, Iowa University, pp. 591-598, 1969.

[52] Tschoegl, Nicholas W., *The Phenomenological Theory of Linear Viscoelastic Behavior: an Introduction*, Springer-Verlag, Berlin Heidelberg, 1989.

[53] United States of Department of Commerce, Tables of the Bessel Functions Y_0, Y_1, K_0, K_1 $(0 \leq x \leq 1)$, *National Bureau of Standards Applied Mathematics Series 1*, Issued February 12, 1948.